

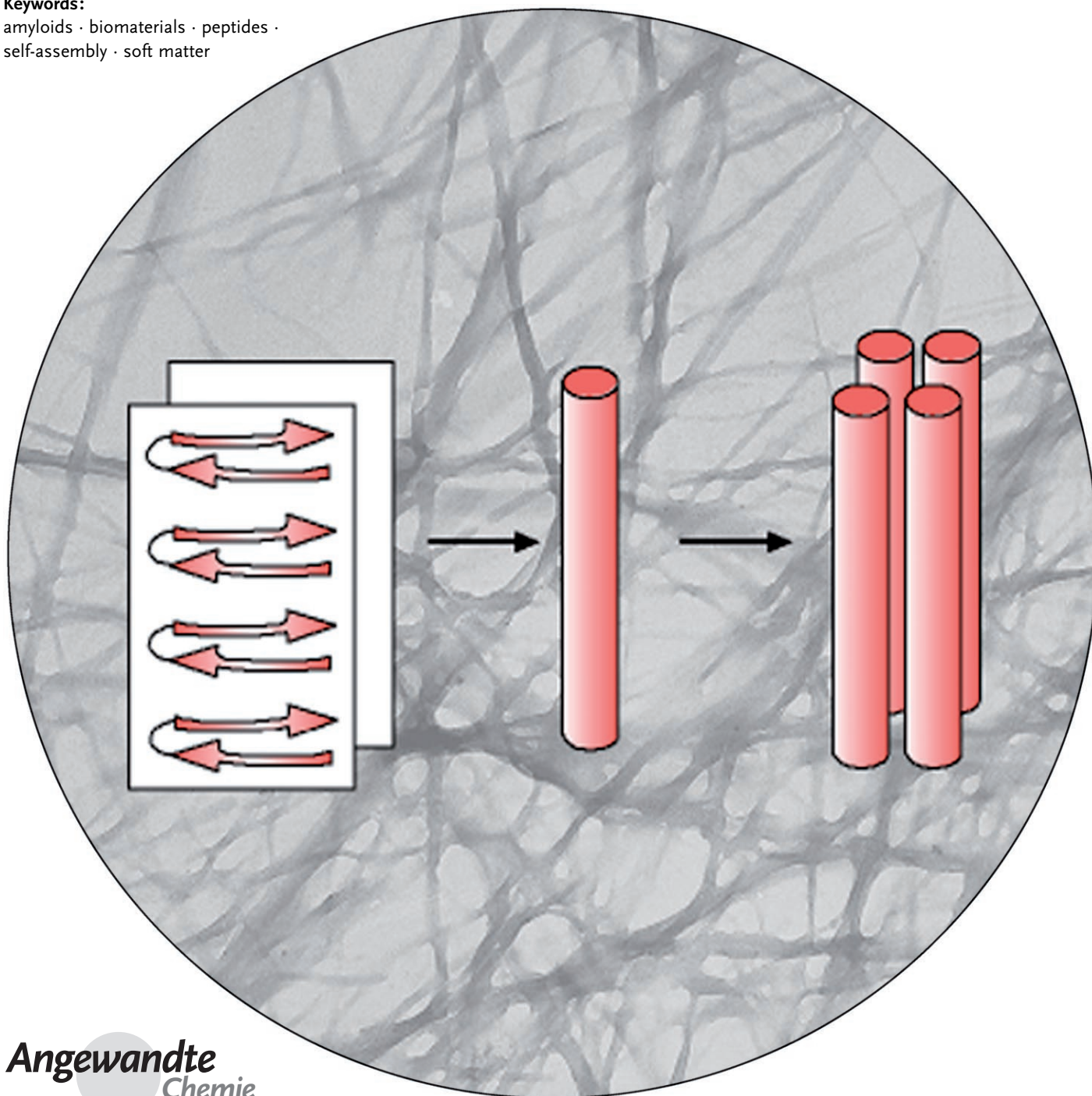
## Fibrillization

DOI: 10.1002/anie.200700861

# Peptide Fibrillization

Ian W. Hamley\*

**Keywords:**  
amyloids · biomaterials · peptides ·  
self-assembly · soft matter



The fibrillization of peptides is relevant to many diseases based on the deposition of amyloids. The formation of fibrils is being intensively studied, especially in terms of nanotechnology applications, where fibrillar peptide hydrogels are used for cell scaffolds, as supports for functional and responsive biomaterials, biosensors, and nanowires. This Review is concerned with fundamental aspects of the self-assembly of peptides into fibrils, and discusses both natural amyloid-forming peptides and synthetic materials, including peptide fragments, copolymers, and amphiphiles.

## 1. Introduction

This Review is concerned with fibril formation by peptides and peptide conjugates, with a focus primarily on amyloid-type fibrils that contain  $\beta$  sheets; other collagen-type fibrillar structures, for example, are not considered. This is a subject of great current interest because of the role of amyloid formation in numerous diseases and the possibilities to use fibrillar peptide structures as structural or structuring elements in bionanotechnology.

The term amyloid refers to protein deposits that resemble those first observed for starch (amyloid originally meant starch-like). It is now specifically associated with proteins and peptides that adopt fibrils based on the cross- $\beta$  structure, in which the peptide backbone is orthogonal to the fibril axis.<sup>[1–5]</sup> The  $\beta$  sheets self-assemble into protofilaments, which may comprise a structure, such as a bundle of twisted  $\beta$ -sheets, which further packs into amyloid fibers<sup>[4,6]</sup> (Figure 1). The

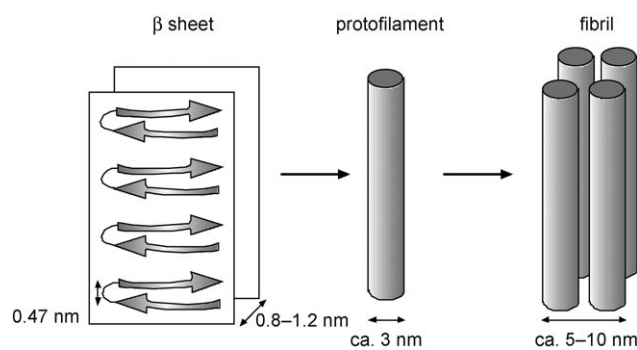


**Figure 1.** Hierarchical structure of amyloid fibrils.

structure of fibrils is discussed further in Section 2. Figure 2 shows a typical TEM image of amyloid fibrils.

The formation of fibrils is symptomatic of many amyloid diseases such as Alzheimer's and Creutzfeldt-Jacob disease<sup>[6,8,9]</sup> (lists of other diseases that result from protein aggregation can be found in Refs. [10,11]). In some species, amyloidosis may be exploited for useful purposes.<sup>[12–14]</sup> In disease, fibrillization results from the aggregation of proteins or peptides such as amyloid- $\beta$  ( $A\beta$ ) or tau. As a consequence of its relevance to a diverse number of conditions affecting

## From the Contents

1. Introduction	8129
2. Structure of Fibrils	8130
3. Characterization of Fibrillization	8131
4. Kinetics (and Mechanism) of Fibrillization	8132
5. Prefibrillar Aggregates Are more Toxic than Final Fibrils	8134
6. Amyloid Formation Is not Sequence Specific	8135
7. Fibrillization of Fragments	8136
8. Fibrillization of <i>de novo</i> Designed Peptides	8137
9. Peptide Amphiphiles and Peptide Copolymers	8138
10. Peptide Nanotubes	8140
11. Peptide Fibrillar Gels	8140
12. Fibrils from $\alpha$ Helices	8142
13. Summary and Outlook	8143

large numbers of people, fibril formation by the  $A\beta$  peptide has been widely studied. There are two variants of this amyloid peptide in humans:  $A\beta_{40}$  and  $A\beta_{42}$  (this notation will be used for the whole peptide with the number of residues indicated), of which the latter forms fibrils more rapidly.<sup>[15]</sup> It is now thought that protofilaments formed in the initial self-assembly process are the toxic agents.<sup>[8,16–21]</sup> This is discussed in more detail in Section 5. The amyloid- $\beta$  peptide (Figure 3) is produced by proteolytic cleavage of the amyloid precursor protein (APP), a transmembrane protein of unknown function.<sup>[8]</sup> The N terminus of the peptide is created by cleavage by  $\beta$ -secretase in the extracellular domain of APP, and the C terminus results from intramembrane cleavage by  $\gamma$ -secretase (Figure 3). A third enzyme,  $\alpha$ -secretase, cleaves between amino acids 16 and 17 in  $A\beta$ , thus hindering fibrillization. Oligomerization of  $A\beta$  occurs intracellularly, as revealed by *in vivo* experiments on human cerebrospinal fluid which

[\*] Prof. I. W. Hamley  
Department of Chemistry  
University of Reading  
Reading, Berkshire RG6 6AD (UK)  
Fax: (+44) 118-378-8450  
E-mail: i.w.hamley@reading.ac.uk

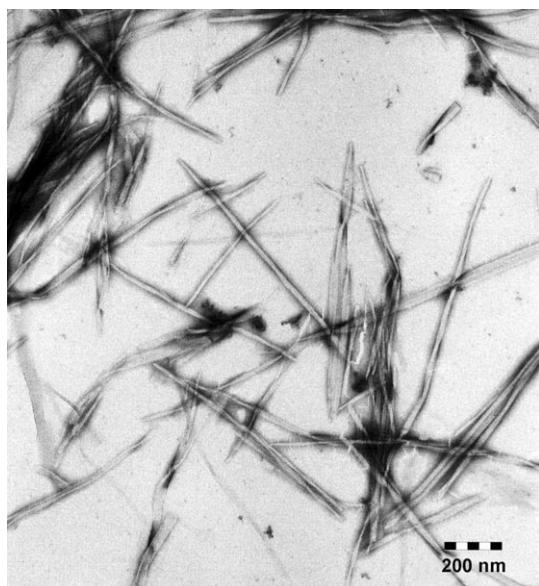


**Figure 2.** TEM image of amyloid fibrils, formed by peptide fragment FFKLVFF.<sup>[7]</sup>



**Figure 3.** Amino acid sequence of A $\beta$ 42. The enzyme cleavage sites are indicated and the polar residues are underlined.

yielded dimers of A $\beta$  that were stable to sodium dodecylsulfate (SDS).<sup>[22]</sup> Incubation did not lead to the production of extracellular oligomers. However, oligomers were detected in neural and non-neural cell lines.

Several genes have been linked to Alzheimer's disease, including the genes for APP,<sup>[23]</sup> presenilin 1 and 2 (PSEN1 and PSEN2),<sup>[24,25]</sup> and apolipoprotein E (APOE).<sup>[26–29]</sup> Recent work suggests that in late-onset Alzheimer's disease, A $\beta$  accumulation occurs intracellularly in late endosomes (i.e. in the deep end of the endosomal compartment) where the enzymes  $\beta$ -secretase and  $\gamma$ -secretase cleave A $\beta$ , the latter in a presenilin-dependent fashion.<sup>[30]</sup> The gene involved in APP



*Ian Hamley, born 1965, is Diamond Professor of Physical Chemistry and head of Physical Chemistry at the University of Reading. He received his PhD from the University of Southampton in 1991. He was then a Royal Society postdoctoral fellow at FOM-AMOLF, Amsterdam, and then in 1992 he carried out postdoctoral research with Frank Bates at the University of Minnesota, Minneapolis. He returned to the UK in 1993 as a lecturer in Physics at the University of Durham, before moving to the Chemistry department at the University of Leeds in 1995, where he became Professor in 2004. He moved to the University of Reading in 2005.*

Leeds in 1995, where he became Professor in 2004. He moved to the University of Reading in 2005.

recycling in endosomes has been identified, and is termed *SORL1* or *LR11*. Normally the protein product of this gene directs APP into recycling endosomes; however, mutations lead to a decrease in the protein product which leads to the pathway where A $\beta$  production is increased by enzymes in the late endosomes. There are several proposed therapies to treat Alzheimer's disease, these are outside the scope of the current review and are discussed elsewhere.<sup>[9]</sup>

The tau protein is involved in microtubule assembly and stabilization within the cytoskeleton (in particular in F-actin fibrils). Mutations can lead to filamentous deposits which have been observed for several neurodegenerative diseases such as Pick's disease and the Parkinsonism-dementia complex of Guam.<sup>[8]</sup> Filamentous tau deposits are invariably present even in the absence of A $\beta$  deposits, and it is not clear in the context of fibril deposition precisely how A $\beta$  and tau interact, although there seems to be a synergistic effect which enhances actin bundling and neurodegeneration.<sup>[8,31]</sup> It has, however, been suggested that, as in the case of A $\beta$ , oligomeric species may be the toxic agents. Neuronal degeneration induced by tau has been studied in vivo. Hyperphosphorylated forms of this microtubule-associated protein induce accumulation of F-actin. This has been confirmed by in vivo studies using drosophila and mouse models.<sup>[31]</sup>

The initial part of this Review focuses on fibrils formed from  $\beta$  sheets. Section 2 describes the structure of fibrils. Section 3 briefly covers methods used to characterize fibrilization. Section 4 discusses aspects of the mechanism and kinetics of self-assembly. Sections 5 and 6 are concerned with the toxicity and sequence specificity of A $\beta$  amyloid formation. Sections 7–10 consider fibril formation with specific types of peptide and peptide conjugates. Section 11 concerns the formation of fibrillar gels. Section 12 briefly summarizes recent work on fibrils formed from coiled-coil peptides. There is finally a summary and outlook.

## 2. Structure of Fibrils

Amyloid fibrils contain bundles of  $\beta$  sheets with backbones orthogonal to the fiber axis in the so-called "cross- $\beta$ " structure.<sup>[1–5]</sup> Figure 4 shows a representation of the cross- $\beta$  structure within a helical fibril constructed from four  $\beta$  sheets. Helical ordering is often observed within the fibrils, for example, for transthyretin,<sup>[32]</sup> the SH3 domain of phosphatidylinositol-3'-kinase,<sup>[33]</sup> or bovine insulin<sup>[34]</sup> (other examples are tabulated in Ref. [5]). The helical structure results from the preferred right-handed twist of  $\beta$  sheets.<sup>[35,36]</sup> The  $\beta$  sheets in the fibrils are antiparallel, as revealed by infrared spectroscopy; an early example of such measurements was made in a study on human amyloid protein.<sup>[37]</sup>



**Figure 4.** Helical packing of a four protofilament bundle proposed for insulin amyloid fibrils. Reprinted with permission from Ref. [34].

Figure 5 shows the  $\beta$  strand-turn- $\beta$  strand conformation of A $\beta$ (18–42) (residues 1–17 are disordered) within the cross- $\beta$  fibril structure. Solid-state NMR experiments (with consideration of the X-ray diffraction and TEM measurements) has indicated a similar structure in A $\beta$ 40.<sup>[38]</sup>

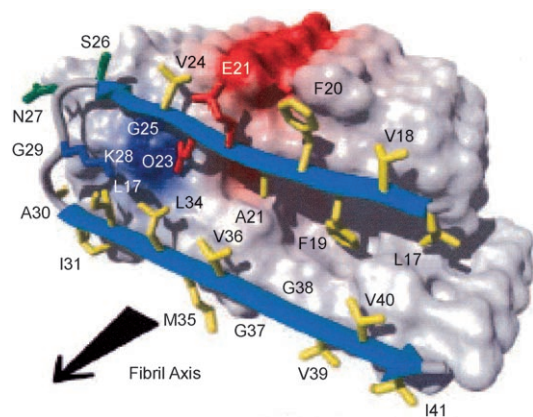


**Figure 5.** Conformation of A $\beta$ (17–42) as revealed by H/D-exchange NMR spectroscopy experiments. The hydrophobic, polar, negatively charged, and positively charged amino acids are shown in yellow, green, red, and blue, respectively. Positively and negatively charged surface patches are shown in blue and red, others in white. Reprinted with permission from Ref. [39].

The characteristic features in an X-ray scattering pattern of the cross- $\beta$  structure are a 4.7 Å meridional reflection corresponding to the spacing between peptide backbones and an equatorial reflection at 8–12 Å, which is broader and which corresponds to the stacking periodicity of the  $\beta$  sheets (the range of values reflects different side-chain dimensions). Most X-ray diffraction studies that showed a cross- $\beta$  structure have been performed on dried films. Since hydration can affect the structure of  $\beta$ -sheet-containing fibrils, Squires et al. have examined whether the cross- $\beta$  structure is retained in flow-aligned solution.<sup>[40]</sup> The wide-angle X-ray scattering (WAXS) results for a synthetic peptide (fragment of transthyretin) and lysozyme from hen egg white indeed showed the same pattern as for a dried sample, thus indicating that the cross- $\beta$  structure is present in solution and is not an artefact caused by dehydration.

Perutz et al. proposed that amyloid fibers are water-filled nanotubes.<sup>[41]</sup> This proposal was based on the analysis of the X-ray diffraction data for the polyglutamine-rich peptide D<sub>2</sub>Q<sub>12</sub>K<sub>2</sub> and for the polyglutamine-rich natural peptides huntingtin and yeast prion Sup35, as well as on an electron microscope image of Sup35. However, this analysis has been challenged by two research groups who have proposed a stacked  $\beta$ -sheet model for the X-ray diffraction data of D<sub>2</sub>Q<sub>12</sub>K<sub>2</sub><sup>[42–44]</sup> (The second research group<sup>[43,44]</sup> also report a stacked  $\beta$ -sheet structure for K<sub>2</sub>Q<sub>28</sub>K<sub>2</sub> and K<sub>2</sub>Q<sub>45</sub>K<sub>2</sub>.) It has also been pointed out that distinctive features in the diffraction patterns of polyglutamine-rich peptides mean that it is very unlikely that the water-filled nanotube model could be a general structure for amyloid fibers.<sup>[42]</sup>

### 3. Characterization of Fibrillization

#### 3.1. Dye Staining

One method for identifying amyloid fibrils is by staining with Congo red. Under polarized light, amyloid samples exhibit green birefringence when stained with Congo red.

Thioflavin T is a fluorescent dye widely used to study amyloid formation. Excitation at 450 nm produces fluorescence at 482 nm.<sup>[45,46]</sup>

#### 3.2. X-ray Diffraction

As mentioned in Section 2, wide-angle X-ray scattering (WAXS) is usually performed on dried samples, in the form of films or “stalks”, the latter being dried threads of solution. Other methods of alignment<sup>[47]</sup> include the use of stretch frames or cryoloops, with the latter producing a dried flat film or “mat”. Stalks may also be dried in the presence of a magnetic field to improve alignment. Small-angle X-ray scattering (SAXS) can provide information on the secondary structure over larger length scales (5–100 nm).

#### 3.3. Dynamic and Static Light Scattering

Analysis of the intensity autocorrelation function of scattered light from a particle undergoing translational or rotational diffusion enables the determination of a diffusion coefficient, and hence, from the Stokes–Einstein equation, the effective hydrodynamic radius. There are several approximate methods to relate this quantity to the fibril length and diameter.<sup>[48,49]</sup>

Static light scattering can be used to obtain the molecular weight of peptide aggregates and also to provide an indication of the particle shape, from measurements of the angular dependence of the scattered intensity.

Light scattering has been used quite widely to monitor the formation of amyloid protofilaments and fibrils.<sup>[50–53]</sup>

#### 3.4. Circular Dichroism

Circular dichroism (CD) refers to the differential absorption of right- and left-circularly polarized light. It is sensitive to the presence of chiral groups and is a primary technique to characterize protein secondary structure. The usual method is based on the “fingerprinting” of features in the 190–250 nm (far-UV) region.<sup>[54]</sup> Data in the near-UV region can provide information on the folding of peptides containing aromatic residues. In the far-UV region, characteristic minima are observed in the absorption spectra at approximately 208 and 222 nm ( $\alpha$  helix), 216–220 nm ( $\beta$  sheet), or 195 nm (random coil). CD spectra are usually analyzed by using algorithms based on databases compiled for peptides for which the X-ray crystal structure is known.<sup>[54]</sup> This permits an accurate determination of the secondary structure, which can then be used to “calibrate” CD spectra. Several algorithms are

available that are based on different databases. Most consider only larger proteins, although there are limited reference data sets (and curve-fitting programs) for shorter peptides.<sup>[55]</sup>

### 3.5. FTIR Spectroscopy

The amide I band of the FTIR spectrum at 1620–1640  $\text{cm}^{-1}$  is associated with  $\beta$  sheets.<sup>[56–60]</sup> In comparison to coils or helices this band is shifted to lower frequency. A further side band at 1680–1690  $\text{cm}^{-1}$  has been ascribed to hydrogen bonding, although *ab initio* calculations<sup>[61]</sup> suggest that it may be due to the vibrational coupling of residues. The narrow intense band observed for some peptides at 1610–1620  $\text{cm}^{-1}$  is ascribed to an antiparallel aggregated structure.

The amide II band around 1550  $\text{cm}^{-1}$  mainly results from the N-H bending vibrations. The frequency of these vibrations are responsive to deuteration (in  $\text{D}_2\text{O}$  the hydrogen atom of the N-H bond exchanges with a deuterium atom) and, as a consequence, the amide II band is shifted by approximately 100  $\text{cm}^{-1}$  to 1450  $\text{cm}^{-1}$ .

Since a full quantum chemical analysis of the vibrational modes of peptides or proteins is not usually possible, the analysis of FTIR data relies on “fingerprinting” or peak-fitting methods.<sup>[56,57]</sup> These methods are prone to uncertainty because of the overlap of features in the spectra.<sup>[56,57,59]</sup>

FTIR measurements can be extended to study linear dichroism on aligned samples with isotope labeling (polarized FTIR) and to vibrational circular dichroism.<sup>[58]</sup>

### 3.6. NMR Spectroscopy

Solid-state NMR spectroscopy has provided much detail on the structure of amyloid fibrils. Various high-resolution experiments employing magic-angle spinning can be performed using  $^{13}\text{C}$ - or  $^{15}\text{N}$ -labeled peptides.<sup>[62–65]</sup> Homonuclear and heteronuclear 2D and 3D spectroscopy may also be performed to give information on interatomic distances and torsion angles for isotopically labeled peptides in the dried state.<sup>[66,67]</sup>

Hydrogen/deuterium exchange techniques have also been employed to probe structural changes during amyloid formation.<sup>[66]</sup> Exchange rates provide information on the structural rearrangements of subsegments of a protein or peptide during folding, unfolding, or fibrillization. This method has also been used to provide a 3D structure for A $\beta$ 42 (see Figure 5).<sup>[39]</sup>

### 3.7. Atomic Force Microscopy and Electron Microscopy

These methods allow the direct imaging of peptide fibrils. Atomic force microscopy (AFM), which is a scanning probe microscopy technique, provides images at the surface. To date, the method has mainly been used to image fibrils from solutions dried onto planar solid substrates such as mica. Electron microscopy includes transmission electron microscopy (TEM) of dried films on holey grids (these are usually

stained with heavy-metal-containing compounds to enhance contrast) or scanning electron microscopy (SEM) of surfaces. Cryotechniques are often preferred as a method to avoid artefacts caused by slow drying.

## 4. Kinetics (and Mechanism) of Fibrillization

Fibrillization appears to occur via a prefibrillar stage<sup>[11,15,50,68,69]</sup> consisting of small (spherical) protein multimers that are consumed as fibrillization proceeds.<sup>[50,68]</sup> AFM studies on A $\beta$ 40 and A $\beta$ 42 provided a compelling picture of the initial formation of protofilaments followed by their replacement with fibrils.<sup>[68]</sup> This technique was complemented with light scattering studies, TEM, and size-exclusion chromatography (SEC) analysis of the molecular weight of fractions obtained at different stages of the polymerization process.<sup>[50]</sup> The aggregation of A $\beta$  on hydrophilic mica and hydrophobic graphite has been investigated. On mica, pseudomicellar aggregates were noted at low concentration, and fibrils at higher concentration. In contrast, on graphite, sheets were observed with a thickness equal to the extended peptide length, oriented along the graphite lattice directions.<sup>[68]</sup> A later AFM study examined A $\beta$ 42 fibrillization and plaque formation, as well as the interaction between A $\beta$ 40 and A $\beta$ 42.<sup>[70]</sup> Deposition was studied on a synthetic template comprising a solid surface activated with *N*-hydroxysuccinimide ester. A $\beta$ 42 oligomers were found to be more effective seeds for fibril growth than monomers or mature fibrils.

The question of whether amyloid fibrillization results from partially folded intermediates containing  $\beta$ -sheet structures or from a fully denatured conformation has recently been addressed. For most proteins, conditions that lead to partial unfolding favor fibrillization. Examples include transthyretin,<sup>[71,72]</sup> the prion protein PrP<sup>C</sup>,<sup>[73,74]</sup> the immunoglobulin light chain,<sup>[75–77]</sup> lysozyme,<sup>[78,79]</sup> the SH3 domain of bovine phosphatidylinositol 3-kinase,<sup>[80]</sup> and  $\beta_2$ -microglobulin.<sup>[81–83]</sup>

The extent of unfolding and ultimately the fibril morphology seem to depend on the level of denaturation.<sup>[82,84]</sup> Kad et al. correlated these two properties in a study of  $\beta_2$ -microglobulin.<sup>[82]</sup> Dobson and co-workers studied the aggregation of acylphosphatase subjected to mild denaturing in aqueous solutions of 2,2,2-trifluoroethanol (TFE) of various concentrations.<sup>[85]</sup> Partial denaturing occurred and led to fibrillization. In contrast, in aggressive denaturing conditions, such as a high concentration of urea or guanidinium chloride, only a soluble highly unfolded state is usually observed. A complication in this study was the fact that the protein has a significant  $\beta$ -sheet content in the native state, and was thus expected to form  $\beta$ -sheet-rich intermediates. A study of fibril formation by myoglobin by the same research group suggested, in contrast, that full denaturing occurs prior to fibrillization.<sup>[86]</sup> Myoglobin is predominately  $\alpha$  helical in its native state and lacks  $\beta$ -sheet content. It is therefore a useful model to study the mechanism of fibrillization. The CD, fluorescence, and FTIR experiments indicated that intermediate states did not contain  $\beta$ -sheet structures. The authors suggested that this partial unfolding mechanism may be generic. This hypothesis supports the evidence that many

proteins lacking specific secondary structure can fibrillize (see Section 6). The intermediate structure must be unfavorable with respect to folding into the native structure, yet must allow non-hydrogen-bonded extended transient structures that may be precursors to amyloid fibrillization.<sup>[85,86]</sup>

Dobson and co-workers as well as other researchers have noted that the unfolded state may contain significant poly(L-proline) II (PPII) content.<sup>[87–89]</sup> Raman spectroscopy studies with polarized light (Raman optical activity) on different forms of synuclein have shown this is not a sufficient condition for  $\beta$ -sheet aggregation, since  $\beta$ - and  $\gamma$ -synuclein have a very limited tendency to form fibrils, despite being rich in PPII.<sup>[90]</sup> By studying A $\beta$ 40 and A $\beta$ 42 in which the methionine (residue 35) side chain was in an oxidized or reduced state, Hou et al. found, from NMR experiments in solution, residue-specific interactions in the early stages of aggregation.<sup>[89]</sup> These studies suggest that both hydrophobic and turnlike structures are required in the first self-assembly steps. The specific region of A $\beta$ 40 involved in contacts between fibrils has been identified by solution-state NMR experiments as corresponding to A $\beta$ (15–24) (other studies on this sequence are discussed in Section 7).<sup>[91]</sup> The NMR data also show that there is an exchange between a monomeric, soluble state and an oligomeric, aggregated state under appropriate (physiological) conditions of salt concentration and that the equilibrium can be shifted by varying the anionic strength. The molecular weight of the oligomer was found to be greater than 100 kDa.<sup>[91]</sup>

Small-angle X-ray scattering (SAXS) has been used<sup>[92]</sup> to monitor the self-assembly of mutant myoglobin with an expanded glutamine repeat sequence (this expansion is associated with diseases such as Huntington's<sup>[93]</sup>). The early stage aggregation was studied upon thermally induced partial unfolding. A nonfibrillar aggregate without characteristic  $\beta$ -sheet features in the X-ray pattern was observed. The authors suggested that this type of protofilament could be related to the toxicity of polyglutamine-rich proteins.

It has been shown that fibrillization is a multistep process and that prefibrillar aggregates formed in the early stages can disassemble.<sup>[94]</sup> Fluorescence experiments were performed on human muscle acylphosphatase under mild denaturing conditions (25% TFE). Partial unfolding occurred to yield globular aggregates 60–200 nm in diameter that could further aggregate into clusters 400–800 nm in diameter. Above a critical concentration of the globular aggregates, larger (> 5  $\mu$ m) superstructures could form. The globular aggregates and clusters disaggregated upon dilution (to 5% TFE). Protein monomers refold quickly whilst globular aggregates and clusters (400–800 nm) disaggregate at a somewhat slower rate. The larger superstructures are not affected by dilution.

Fibrillization of A $\beta$ 40 occurs above a critical concentration, which has been described in analogy with a critical micelle concentration.<sup>[48,95,96]</sup> Figure 6 is identical in form to that for micellization.<sup>[97]</sup> Fibrillization can be described using the corresponding one-dimensional model of self-assembly.<sup>[97]</sup>

It is commonly observed that fibrillization occurs after a lag phase, which suggests a nucleation and growth process.<sup>[48,82,95,96,98–101]</sup> The lag phase can be eliminated by addition of preformed aggregates, that is, by seeding (Figure 7).<sup>[95,96]</sup>

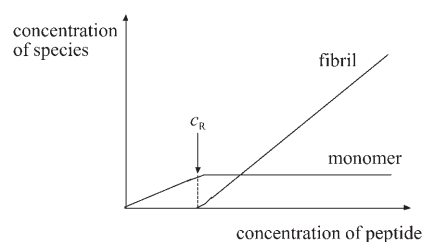


**Figure 6.** The amount of fibril and monomer as a function of added protein. Fibrils are formed above a critical concentration  $c_R$ .

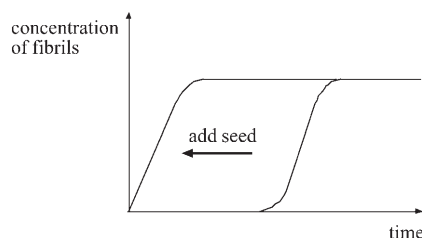


**Figure 7.** The addition of seed can eliminate the lag time in fibrillization.

The initially formed protofibrillar species for several proteins including A $\beta$ 40, A $\beta$ 42, and  $\alpha$ -synuclein are spherical, porelike, annular species,<sup>[11,68,69]</sup> which may be linked into chains.<sup>[11,69]</sup> The protofibril formation process may occur before or during the lag phase.

Fibril formation from hen egg white lysozyme (HEWL) induced at low pH values and high temperature (57 °C) occurs after an extended lag time of 48 h. The lag time is independent of concentration, which indicates that fibril formation is a single-molecule process.<sup>[84]</sup> The observation of an isodichroic point in the CD data points to a two-state cooperative process as the initial  $\alpha$ -helix-rich structure unfolds. CD measurements on fractions separated by filtration from a sample heated for 11 days showed that the monomer had a random coil structure and the fibrils were characterized by an additional small  $\beta$ -sheet signal. It was noted that the fibril morphology is dependent on the preparation conditions.

In contrast to the lag time observed with HEWL, aggregation of  $\beta$ -lactoglobulin occurs immediately upon heating.<sup>[102]</sup> This finding points to distinct mechanisms of fibrillization. A possible factor is the  $\beta$ -sheet content in the protein, since  $\beta$ -lactoglobulin is rich in this secondary structure whereas HEWL is rich in  $\alpha$ -helix structures (30–40%<sup>[103,104]</sup>). The suggested mechanism for heat-induced fibrillization of  $\beta$ -lactoglobulin involves several steps: First, the incorporation of (partly) denatured protein molecules into fibrils or nonfibril-forming oligomers. A second step involves the reversible formation of linear aggregates, followed by a third process of “consolidation”, which produces thermally stable fibrils.<sup>[102]</sup>

The structure of  $\beta$ -lactoglobulin aggregates produced by heat-induced denaturation at pH 2 has been probed by light and neutron scattering studies.<sup>[105]</sup> The morphology was found

to depend on the ionic strength, thereby pointing to the role of electrostatic interactions in the self-assembly process. Rodlike aggregates were observed at low ionic strength, whereas a fractal structure was suggested for solutions at higher ionic strength. A two-step aggregation process was not observed at pH 2, where fibrils form, but was seen at pH 7 where globular aggregates form.<sup>[105]</sup>

The dependence of the morphology on the ionic strength was later probed by AFM and light scattering experiments.<sup>[106]</sup> A critical concentration for fibril formation was reported and it was also noted that fibrils became shorter and more curved on increasing the ionic strength. The formation of fibrillar gels by  $\beta$ -lactoglobulin at high concentration is discussed in Section 11. As mentioned above, the lag time observed in fibrillization can be eliminated or greatly reduced by seeding with preformed fibrils.<sup>[6,107]</sup>

The role of shear flow on amyloid formation has been investigated by fluorescence experiments on  $\beta$ -lactoglobulin and by AFM studies on extracted aliquots.<sup>[108]</sup> Shear-induced formation of spheroidal aggregates was observed in a couette cell (concentric cylinder). These aggregates could be used to seed subsequent fibrillization by incubation; the fibrillization was significantly enhanced relative to the unseeded control solution. Preformed fibrils were degraded into shorter fibrils during prolonged steady shear at a high shear rate. These results were placed in the context of physiological blood-flow conditions.<sup>[108]</sup> SAXS, TEM, and dynamic light scattering (DLS) studies also provide evidence for the break-up of  $\beta$ -lactoglobulin into short rodlike fragments after continuous shear (alignment is observed in the early stages of flow).<sup>[109]</sup>

Early work on the growth phase of fibrillization in A $\beta$ 40 suggested that the kinetics are first order, that is, the rate of fibril elongation is proportional to the concentration of the monomers.<sup>[48,110,111]</sup> This was confirmed by light scattering studies on A $\beta$ 40 in 0.1M HCl<sup>[48]</sup> (the aggregation kinetics are pH-dependent), in vitro studies of deposition onto plaques in brain tissue of Alzheimer's patients,<sup>[110]</sup> and thioflavin T (ThT) fluorescence studies.<sup>[111]</sup> The temperature-dependence of aggregation for A $\beta$ 40 (determined from size measurements by dynamic light scattering) follows the Arrhenius equation,<sup>[51]</sup> with an activation energy of 96 kJ mol<sup>-1</sup> that is comparable to the value for the unfolding of several other peptides.<sup>[51]</sup> As mentioned above, the kinetics of dilution-induced disaggregation has been probed for monomers and early stage protofilaments of human muscle acylphosphatase.<sup>[94]</sup> More recent work indicates that the kinetics of fibrillization are more complex, with a sigmoidal shape of the growth curve.

Two research groups have investigated the kinetics of fibrillization of yeast prion protein Sup35.<sup>[112,113]</sup> The growth kinetics following seeding could be interpreted using a three-step model involving nucleation, stepwise monomer addition, but also fragmentation of fibrils.<sup>[112]</sup> In other words, as well as the assembly of fibrils by monomer addition there is a competing disassembly process. A molecular chaperone was shown to disaggregate Sup35 by subtraction of oligomers (hexamers to dodecamers).<sup>[113]</sup> These results point to the importance of low-molecular-weight oligomers in the assembly and disassembly of fibrils.

The rate of fibrillization is strongly influenced by seeding.<sup>[95]</sup> The efficiency of seeding appears to be correlated to the similarity in sequence between the added protein and the seeded protein, as shown by experiments where fibrils of various proteins were added to a solution of hen lysozyme.<sup>[114]</sup> Fibril morphology is also influenced by seeding, as revealed by TEM and solid-state NMR studies on A $\beta$ 40.<sup>[115]</sup> It is also reported that preparation conditions, in particular, the use of sonication, affect both fibril morphology and toxicity.<sup>[115]</sup> AFM studies on  $\beta$ -lactoglobulin<sup>[102,116]</sup> and HEWL<sup>[84]</sup> have shown that morphology is strongly affected by the preparation conditions, where unfolding is induced by the pH value, solvent, or heat.

It has been reported that the aggregation rate is correlated to fibril length.<sup>[83]</sup> Fast aggregation is associated with short fibrils, whereas conditions favoring slower growth lead to longer fibrils. On the other hand, more recent ThT fluorescence studies indicate that the seed-induced growth kinetics of  $\beta_2$ -microglobulin varies from fibril to fibril, although growth is always unidirectional and first order.<sup>[117]</sup> This result may reflect variations in the  $\beta$ -sheet configuration at the growth front.

## 5. Prefibrillar Aggregates Are more Toxic than Final Fibrils

It is now thought that protofilaments formed in the initial self-assembly process of A $\beta$  are the toxic agents.<sup>[8,15-21,118-124]</sup> Evidence for this comes from several experiments on disease-related and nondisease-related proteins. In vivo and cell culture experiments showed that A $\beta$ 42 oligomers, formed under conditions that inhibited fibril formation, were neurotoxic.<sup>[118-120]</sup> Oligomeric forms of A $\beta$ , specifically dimers and trimers, were shown to disrupt learning behavior in rats.<sup>[124]</sup> Anti-A $\beta$  antibodies isolated from immunoglobulin strongly disrupt fibrillization.<sup>[125]</sup> Polyclonal antibody experiments indicate that antibodies suppress the toxicity of soluble oligomers, whereas there is no antibody response to mature fibrils.<sup>[122]</sup> This behavior has been proposed as a possible starting point for the development of a vaccination using A $\beta$ 42 oligomers.<sup>[126]</sup> Experiments on A $\beta$ ,  $\alpha$ -synuclein, and transthyretin suggest that cytotoxicity shares a common cause not related to the specific sequence (see the discussion in Section 6 on the common origin of amyloid aggregation).<sup>[16,21]</sup> For example, two proteins (unrelated to disease)—the N-terminal HypF-N domain of *E. coli* and the SH31 domain from bovine phosphatidylinositol 3-kinase—have been shown to be toxic to cells only when added to the culture medium in prefibrillar form.<sup>[16]</sup> Recent in vivo studies on a mouse model suggest that specific soluble A $\beta$  multimeric species, specifically dodecameric 56 kDa species, are associated with memory loss in Alzheimer's disease.<sup>[127]</sup>

The mechanism of cytotoxicity may be related to the fact that several amyloidogenic proteins and peptides have been shown to form membrane pores or channels.<sup>[18,128-130]</sup> This could be due to the exposure of hydrophobic regions in misfolded proteins, such as those that form amyloid fibrils.<sup>[129]</sup> The presence of positive charge on a peptide which enables

interaction with negatively charged lipid membranes may also be important.<sup>[129]</sup> According to the channel hypothesis, pore formation is responsible for the neurotoxicity of A $\beta$ . The original work by Arispe et al.<sup>[131–133]</sup> established that A $\beta$  is capable of forming membrane channels. Lambert et al. showed that A $\beta$ 42 oligomers bind to cell membranes and cause cytotoxicity under conditions in which mature fibrils do not form.<sup>[118]</sup> Further support for this result is the finding that pore formation is inhibited by the binding of Congo red,<sup>[134]</sup> which indicates that the A $\beta$  needs to be aggregated into (proto)filaments for this mechanism to be effective. AFM studies have revealed that A $\beta$  forms pores in lipid membranes that contain multimers of the protein.<sup>[135]</sup> Uptake of Ca<sup>2+</sup> across the ion channels leads to neuritic degeneration and ultimately cell death.<sup>[135]</sup> This mechanism was also

implicated for the N-terminal Hyp-F domain and suggests that it is common to several amyloid-forming peptides, including those not related to disease and those involved in several rare degenerative diseases.<sup>[21]</sup> Protofibrillar variants of  $\alpha$ -synuclein (known to be linked to certain forms of Parkinson's disease) were shown to exhibit enhanced permeability across phospholipid vesicle membranes relative to that of the wild-type protein.<sup>[136]</sup> Selective leakage of low-molecular-mass molecules suggested poration of the vesicles.<sup>[136]</sup> The intracellular Ca<sup>2+</sup> concentration and redox status of the Hyp-F N-terminal domain was studied by fluorescence experiments. The cytotoxicity behavior caused by an increase in free Ca<sup>2+</sup> ions and reactive oxygen species is similar to that for proteins involved in specific amyloidoses<sup>[18]</sup> and consistent with the conclusion, discussed above, that aggregation and resultant cytotoxicity is not sequence specific (Section 6).<sup>[21]</sup>

The importance of “gatekeeper residues” that cap aggregation-prone sequences in natural proteins and help to hinder aggregation into fibrils has been highlighted.<sup>[17]</sup> There is clearly scope for evolutionary pressure to ensure that proteins contain residues that hinder aggregation and/or promote folding into the native state.<sup>[17,100]</sup> Specific residues that oppose aggregation were analyzed using a computer algorithm that analyzes the aggregation propensity of sequences.<sup>[17]</sup>

The toxicity of A $\beta$ 42 is much greater than A $\beta$ 40<sup>[119,123]</sup> because of its greater tendency to fibrillize, as mentioned in Section 2. It is unclear whether extracellular or intracellular processes are responsible for the toxicity of A $\beta$ . Intracellular A $\beta$ 42 is neurotoxic, at least for human neurons.<sup>[123]</sup> The observation that protofilaments are more toxic than mature aggregates also seems to be the case for tau.<sup>[8]</sup>

Figure 8 shows the proposed pathways for in vivo aggregation of A $\beta$ 42 that are relevant to age-related proteotoxicity.<sup>[19]</sup> The insulin/insulin growth factor-1-like signaling (IIS) pathway is regulated by the receptor DAF-2 (inhibition of

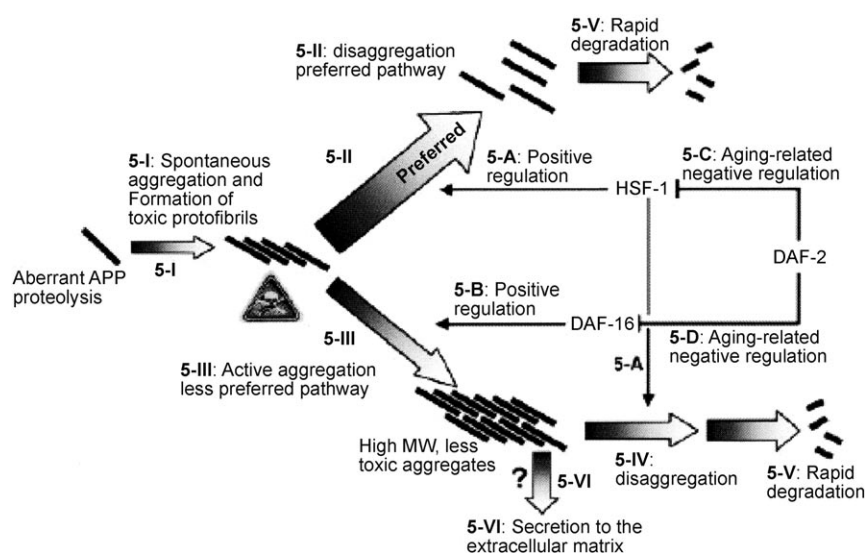


**Figure 8.** Schematic representation of the regulation pathways of fibrillization in age-onset A $\beta$  proteolysis. (Reprinted with permission from Ref. [19]. Copyright 2006, American Association for the Advancement of Science (AAAS).)

DAF-2 expression extends the lifespan of worm models). The two transcription factors heat shock factor (HSF-1) and DAF-16 regulate the opposing disaggregation and aggregation processes. The preferred mechanism whereby toxic aggregates are rapidly degraded (5-II) is positively regulated by HSF-1 (stage 5-A) and negatively regulated by DAF-2 (stage 5-C). When the HSF-1-regulated disaggregation mechanism is overloaded, a second mechanism comes into play (5-III). This produces less toxic higher molecular weight aggregates. This is positively regulated by DAF-16 (stage 5-B) and negatively by DAF-2 (stage 5-D). The high-molecular weight aggregates can be eliminated by several methods, as indicated in Figure 8.

## 6. Amyloid Formation Is not Sequence Specific

The cross- $\beta$  structure (Section 2) seems to be a common feature for amyloids formed by many different proteins and peptides.<sup>[18,20,137]</sup> Evidence that the formation of amyloid fibrils is a common state for many, if not all, proteins comes from several types of experiments: First, fibrils can be induced to form by partial denaturing of proteins not involved with any disease<sup>[85]</sup> or using de novo designed peptide fragments (see Section 8). Second, amyloids can be induced to form by seeding with fibrils of the same, related, or unrelated protein.<sup>[82,96,99,107,114,138]</sup> This process may be implicated in the transmission of prion diseases,<sup>[96]</sup> although the transmission of spongiform encephalopathies may involve cofactors in addition to prions—the full mechanism is unclear at the moment.<sup>[139]</sup> Small peptide fragments can be designed to inhibit fibrillization; in particular, fragments containing sequences homologous to A $\beta$ 40 can inhibit its fibrillization, as discussed in Section 7.

Fändrich and Dobson showed that cross- $\beta$  structures could be formed independently of the sequence or side-chain

type for a series of polyamino acids, for example, poly(L-lysine), poly(L-glutamic acid), and poly(L-threonine).<sup>[140]</sup> They point out that this is quite distinct to protein folding, which depends on the specificity of side-chain interactions. However, under certain conditions (of temperature or pH), aggregation in amyloid fibrils can be overcome by specific side-chain interactions, which may lead to kinetically favorable states or may destabilize fibrillar aggregates. It thus appears that fibril formation is due to the common main-chain polypeptide backbone whereas folding is due to specific interactions of the side chains.<sup>[100]</sup>

Amyloids also have the common property that they are stained by Congo red and thioflavin dyes. This may simply reflect the common cross- $\beta$  structure.<sup>[18]</sup> Glabe and co-workers studied an antibody that is specific to soluble oligomeric intermediates of A $\beta$  and showed that it also recognizes oligomers from a range of other proteins and peptides.<sup>[122]</sup> Recognition was not observed for low-molecular-weight or fibrillar A $\beta$  species. This finding indicates that the antibody recognizes a common epitope in soluble oligomers.

In recent work, mutants of wild-type A $\beta$ 42 have been prepared in which hydrophobic residues in the C terminal half were substituted with random nonpolar residues.<sup>[141]</sup> It was shown that fibrillization was unaffected. This finding implies that generic hydrophobic sequences are sufficient to promote A $\beta$ 42 fibrillization.

## 7. Fibrillization of Fragments

Recent work has focussed on determining the minimal peptide sequence that can still exhibit amyloid-type fibrillization.<sup>[44]</sup> Much work has focused on A $\beta$ , as discussed in the following. However, the minimal core domain sequence has also been determined for the PHF6 tau protein (VYK),<sup>[142]</sup> medin (NFGSVQ),<sup>[143]</sup> human calcitonin (DFNK),<sup>[144]</sup> and yeast prion Sup35 (GNNQQNY).<sup>[138]</sup> It is interesting that core domains can be as short as three amino acids.

The fibrillization of fragments of A $\beta$ 40 and A $\beta$ 42 has been investigated extensively. Several early studies are summarized in the reviews by Teplow<sup>[6]</sup> and Serpell.<sup>[4]</sup> In this section, the focus is on fibrillization by the shortest fragment which is critical for fibril formation. Hilbich et al. showed that a region in the hydrophobic core around residues 17 to 20 (that is, LVFF) is crucial for  $\beta$ -sheet formation.<sup>[145]</sup> They prepared variants of A $\beta$ 42, by various substitutions of residues 17 to 20, and investigated fibrillization by CD, FTIR, and TEM experiments. Substitution with hydrophilic amino acids led to a significant reduction in amyloid formation. Tjernberg et al. studied the binding of fragments and variant fragments of A $\beta$ 40 to the full peptide.<sup>[146,147]</sup> The binding of <sup>125</sup>I-labeled A $\beta$ 40 was studied by autoradiography. A series of fragments of A $\beta$ 40 ranging from 3 to 10 residues was prepared. Only pentapeptides or longer showed significant binding to A $\beta$ 40, and fragment A $\beta$ (16–20) (that is, KLVFF) is contained in all strongly binding sequences.<sup>[147]</sup> By preparing pentapeptide variants of KLVFF with substituted amino acids, it was found that residues 2,3, and 5 (K,L,F) are most important for the binding of this fragment to A $\beta$ 40.<sup>[146,147]</sup> A model for the

binding of KLVFF to A $\beta$ (13–23) confirmed the importance of these residues in forming an antiparallel  $\beta$  sheet. The binding capacity of pentapeptides containing D-amino acids instead of L-amino acids was also studied, since the latter are resistant to proteolysis. Residues 2 and 3 were found to be most critical for binding, with D-Lys and D-Phe enhancing the binding.<sup>[147]</sup> Findeis et al. reported the inhibition of A $\beta$  fibrillization by A $\beta$  fragments.<sup>[148]</sup> This study revealed once again the importance of the A $\beta$ (16–21) region. A derivative of A $\beta$ (17–21), namely cholyl-LVFFA-OH, was found to be a particularly potent inhibitor of fibrillization, although with limited biochemical stability. The D-amino acid version, however, was found to be stable in monkey cerebrospinal fluid.

The dependence of fibrillization on the fragment size was investigated for A $\beta$  fragments containing the A $\beta$ (16–20) sequence.<sup>[149]</sup> Electron microscopy studies suggested that the shortest fibril-forming sequence was A $\beta$ (14–23) (that is, the decapeptide HQKLVFFAED). The KLVFF sequence was found not to form fibrils itself. Meredith and co-workers later studied variants of KLVFF<sup>[150]</sup> and KLVFFAE<sup>[151]</sup> in which the amide protons in alternate residues were replaced by *N*-methyl groups.<sup>[150,151]</sup> Ac-K(Me)LV(Me)FF-NH<sub>2</sub> was shown to form extended  $\beta$  strands.<sup>[150]</sup> It is also more water soluble than KLVFF, can permeate phospholipid vesicles and cell membranes, and is resistant to denaturation by the addition of solvent or by an increase in temperature or pH value. It is also a potent inhibitor of A $\beta$ 40 fibrillization, and can break up preformed A $\beta$ 40 fibrils; it is more effective than KLVFF in both processes<sup>[150]</sup> (as is heptapeptide NH<sub>2</sub>-KLV(Me)F(Me)F(Me)A(Me)E-CONH<sub>2</sub><sup>[151]</sup>).

These fragments are believed to form  $\beta$  strands with distinct faces: one with unmodified groups capable of forming hydrogen bonds and the other containing nonpolar methyl groups. This arrangement can disrupt the hydrogen-bonded  $\beta$ -sheet structure of the A $\beta$  peptide itself. Other fragments have been designed to inhibit A $\beta$ 40 and A $\beta$ 42 fibrillization. Rational design principles based on the knowledge of the pentapeptide binding sequence led to a study on LPFFD.<sup>[152]</sup> This peptide incorporates proline, which is known to be a  $\beta$ -sheet blocker, and was found to reduce amyloid deposition in vivo and to disassemble preformed fibrils in vitro.<sup>[152]</sup> It has been reported<sup>[153]</sup> that the retro-inverse peptide fflvk (lower case indicates D-amino acids) binds A $\beta$ 40 fibrils with moderate affinity, but that this binding can be significantly enhanced by attaching multiple copies of this peptide to an eight-arm branched poly(ethylene glycol) (PEG). Tandem dimers of fflvk linked by a k( $\beta$ A) spacer or a difunctional PEG chain also showed some enhancement of binding. All of these conjugates are effective in inhibiting fibrillization of the full A $\beta$ 40 peptide.<sup>[153]</sup>

TEM studies indicated that KLVFF itself forms fibrils in aqueous phosphate-buffered saline (PBS) solutions (pH 7.4),<sup>[150]</sup> which is contrary to the reports by Tjernberg et al.<sup>[149]</sup> There is, therefore, some controversy as to whether this fragment itself fibrillizes. In a separate study, fibril formation has been reported for the heptapeptide A $\beta$ (16–22) (that is, (CH<sub>3</sub>CO-)KLVFFAE(-NH<sub>2</sub>)).<sup>[154]</sup> It has been suggested on the basis of electron microscopy, atomic force microscopy, and small-angle scattering data that fibrils of this

peptide actually comprise nanotubes.<sup>[155]</sup> Analysis of the 3D structure of A $\beta$ 42 obtained from NMR measurements suggests that residues A $\beta$ (18–26) form a  $\beta$ -sheet structure, as do residues 31–42, within the overall  $\beta$ -strand-turn- $\beta$ -strand structure of residues 18–42 (Figure 5; residues 1–17 are disordered).<sup>[39]</sup> The A $\beta$ (17–23) sequence, which seems to be vital for amyloid self-assembly, has also been shown to be important in forming the correct  $\beta$ -pleated sheet structure of the A $\beta$  peptide.<sup>[145,156]</sup>

Computer modeling studies based on the calculation of the partition functions of  $\beta$ -sheet peptide configurations predicts that A $\beta$ (17–21) should be prone to  $\beta$ -sheet aggregation.<sup>[17,157]</sup> Algorithms based on the analysis of the aggregation properties of the constituent amino acids also predict aggregation for this region of A $\beta$ (1–42).<sup>[158]</sup> On the basis of results obtained by using a similar methodology, Kallberg et al.<sup>[159]</sup> suggest that A $\beta$ (16–23) is a so-called discordant sequence of amino acids, in the sense that this sequence is predicted to adopt a  $\beta$ -strand conformation, whereas the full protein structure in the protein database (Ref. 1ba6) indicates an  $\alpha$  helix for this region of A $\beta$ 40. The protein database structure 1ba6<sup>[160]</sup> is for A $\beta$ 40 with oxidized methionine (residue 35) in aqueous SDS solution, a solvent which is known to favor  $\alpha$  helices.

NMR spectroscopic data on A $\beta$ 40 in water/TFE solution<sup>[161]</sup> and in SDS solution<sup>[162]</sup> also indicate an  $\alpha$  helix for residues 15–24 in aqueous solution (data from Sticht et al.<sup>[161]</sup> corresponding to pdb structure 1 AML). As mentioned above, NMR studies in aqueous solution<sup>[39]</sup> indicates a  $\beta$ -sheet structure in this region of A $\beta$ 42. Other methods that predict secondary structure indeed lead to different predictions for the conformation of KLVFF.<sup>[163]</sup> The method of Garnier predicts  $\alpha$  helices for KLVFF, whereas the Chou–Fasman method predicts residues KLV are in  $\beta$ -strand and FF in  $\alpha$ -helix structures.

Sequences in this central region of A $\beta$ 42 are also of great interest because cleavage by the enzyme  $\alpha$ -secretase occurs between K and L.<sup>[8]</sup> The cleaved peptide fragments do not undergo fibrillization.

## 8. Fibrillization of de novo Designed Peptides

The self-assembly of two types of de novo designed peptides has been studied extensively by Aggeli et al. Peptides K24 and K27 (the numbers indicate the numbers of the residues) are related to the transmembrane domain of the IsK protein and were designed to form  $\beta$  sheets in organic solvents.<sup>[164,165]</sup> The second series of peptides prepared were 11-residue peptides designed to form  $\beta$  sheets in water.<sup>[166]</sup> The original peptide (DN1 or P<sub>11</sub>-II) contained six glutamine residues that provided a hydrophobic face to the  $\beta$  sheet, and other residues that provided a hydrophilic surface.

The self-assembly of K24 into  $\beta$  sheets was studied and the gelation in sufficiently polar solvents was probed.<sup>[164,166]</sup> Gel diagrams were compiled and the dependence on the parameters solvent polarity (dielectric constant) and hydrogen-bonding ability determined. The rheological properties of the gels were investigated, and a strong increase in the modulus

was observed following pre-shear. The structure of the self-assembled tapes formed by K24 in 2-chloroethanol was investigated in detail by dynamic light scattering studies.<sup>[167]</sup> Networks above the critical gel concentration were described in terms of entangled semirigid polymers.

The self-assembly of peptides such as DN1 was analyzed using a model<sup>[168]</sup> that accounts for the energy of interaction between monomers ( $\beta$  strands), tapes ( $\beta$  sheets), and ribbons (stacks of  $\beta$  sheets) as well as the elastic penalty for twisting ribbons into helices. Figure 9 provides a schematic representation of the hierarchical self-assembly as well as a calculated phase diagram.

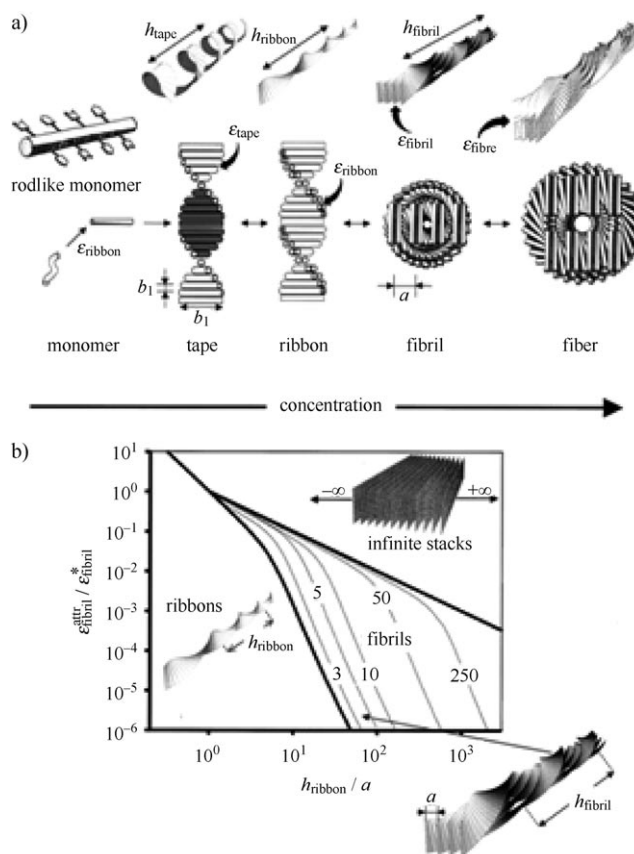


**Figure 9.** Self-assembly of chiral peptide tapes.<sup>[169]</sup> a) Successive stages in the self-assembly process are illustrated, and the associated interaction energies  $\varepsilon$  are indicated. b) Calculated phase diagram in terms of the parameters  $\varepsilon_{\text{fibril}}^{\text{attr}}/\varepsilon_{\text{fibril}}^*$  (relative side-by-side attraction energy between ribbons) and  $h_{\text{ribbon}}/a$  (the relative helix pitch of ribbons). The thick lines divide regions where different aggregates are stable. The dotted lines are lines of stability for fibrils containing  $p$  ribbons. The calculation<sup>[168]</sup> was performed for a ratio of the elastic constants  $k_{\text{bend}}/k_{\text{twist}} = 0.1$ .

The influence of amino acid substitutions on the self-assembly of peptides with 11 amino acids based on DN1 into fibrils has been examined. The substitutions affect the charge and hydrophobicity of the peptides. Changes in the fibril length, width, and aggregation state were noted.<sup>[170]</sup> Later, internal dynamics were studied by dynamic light scattering.<sup>[170]</sup> The formation of nematic gels was also investi-

gated.<sup>[169–172]</sup> A fluid–fluid isotropic–nematic phase transition occurs as the concentration is increased; a transition between viscoelastic and gel nematic states is observed at higher concentration.<sup>[169]</sup> Gelation can be switched very rapidly (within seconds) by variation of the pH value when DN1-type peptides are designed with appropriate sequences.<sup>[172]</sup>

A series of de novo designed hexapeptides were prepared on the basis of computer database searching of sequences with a propensity to form  $\beta$  sheets.<sup>[173]</sup> It was found that fibrillization only occurred if the charge on the peptide was +1 or –1. The peptides assembled into a cross- $\beta$  structure with four antiparallel  $\beta$  sheets running parallel to the axis of the protofilaments, similar to the model of Blake and Serpell<sup>[32]</sup> (although there was no evidence for the twisting of  $\beta$  sheets).

Chen has studied the self-assembly of a range of so-called ionic complementary peptides into fibrils.<sup>[174]</sup> These contain sequences of alternating positively and negatively charged peptides of several sequence types such as –+ (type I) ––++ (type II), and ––––++++ (type IV); one example is AEAEAKAKAEAEAKAK (type II). Other peptides studied are listed in Ref. [174]. The self-assembly of these peptides depends on the sequence<sup>[175]</sup> and is also susceptible to pH changes and added salt counterions.<sup>[174]</sup> The addition of copper salts was shown to change the conformation of a type II peptide with a metal-ion-binding GGH end group from an  $\alpha$ -helix/random coil to a  $\beta$ -sheet structure.<sup>[176]</sup> AFM studies have shown that different anions change the fibril morphology: Divalent  $\text{SO}_4^{2-}$  ions led to long fibrils, whereas monovalent counterions such as  $\text{Cl}^-$  and  $\text{NO}_3^-$  led to short fibrils.<sup>[176]</sup> It was suggested that the divalent anion could form an electrostatic bridge between the K units and lead to fibrils. In the case of the monovalent anions, there was evidence for a mixed secondary structure, including  $\alpha$ -helix/random coil that could disrupt fibrillization.<sup>[176]</sup> Other research groups have designed peptides that undergo conformational changes to form  $\beta$  sheets upon binding metal ions.<sup>[177,178]</sup>

The self-assembly of a series of amphiphilic  $\beta$ -sheet peptides of the form PK- $X^1$ -K- $X^2$ - $X^2$ -E- $X^1$ -EP, where  $X^1$  and  $X^2$  are hydrophobic residues (F, I, V, or Y), has been investigated.<sup>[179]</sup> Several variants with aromatic  $X^1$  and  $X^2$  residues were shown to form helical ribbons which aggregated into straight fibers, as in the model introduced by Aggeli et al.<sup>[169]</sup> However, variants with only aliphatic side groups formed tapelike fibers, with no evidence of helical stacking within the fibrils. Considering the propensity of amino acids to form  $\beta$  sheets, I and F were shown to strongly favor fibrillization, whereas peptides containing a VV sequence or one or two tyrosine units did not form fibrils. Tyrosine is not very hydrophobic and these findings highlight the role of hydrophobicity in the self-assembly process.<sup>[179]</sup>

## 9. Peptide Amphiphiles and Peptide Copolymers

Peptide amphiphiles (PAs) and copolymers are related structures. PAs usually comprise a hydrophilic peptide to which a hydrophobic tail is attached—this may be a hydrocarbon chain or a sequence of hydrophobic amino acids. Self-assembly drives these surfactants to form typical structures

such as micelles and vesicles, but nanotubes are also formed (discussed in Section 10). Block copolymers containing peptide units may have hydrophilic or hydrophobic synthetic polymers conjugated to peptide sequences of opposite amphiphilicity in architectures that include diblocks, triblocks, etc. Most work has been on conjugates of peptides with hydrophilic poly(ethylene glycol) units.

Stupp and co-workers designed PAs with multiple functional building blocks which self-assembled into nanofibers and which could be used to fabricate biomaterials, such as scaffolds for biomineralization.<sup>[180,181]</sup> The PAs (Figure 10) comprised a hydrocarbon tail group (region 1) attached to a unit with four cysteine residues (to enable cross-linking through formation of disulfide bonds, region 2); a flexible region (3) of three G residues linked the head group to the cross-linked region. The head group itself comprised a single phosphorylated serine residue (4) attached to an RGD cell-binding ligand (5). The phosphorylated serine residue was designed to interact with  $\text{Ca}^{2+}$  ions and to help direct mineralization of hydroxyapatite during biomineralization. These PAs were shown to self-assemble reversibly at low pH values.<sup>[180]</sup> The influences of amino acid sequence and modification of the alkyl tail on fibril morphology were also investigated.<sup>[181]</sup> Gelation was observed upon addition of divalent cations, and fibril formation at pH 8 was observed on drying, thus pointing to the role of concentration in the self-

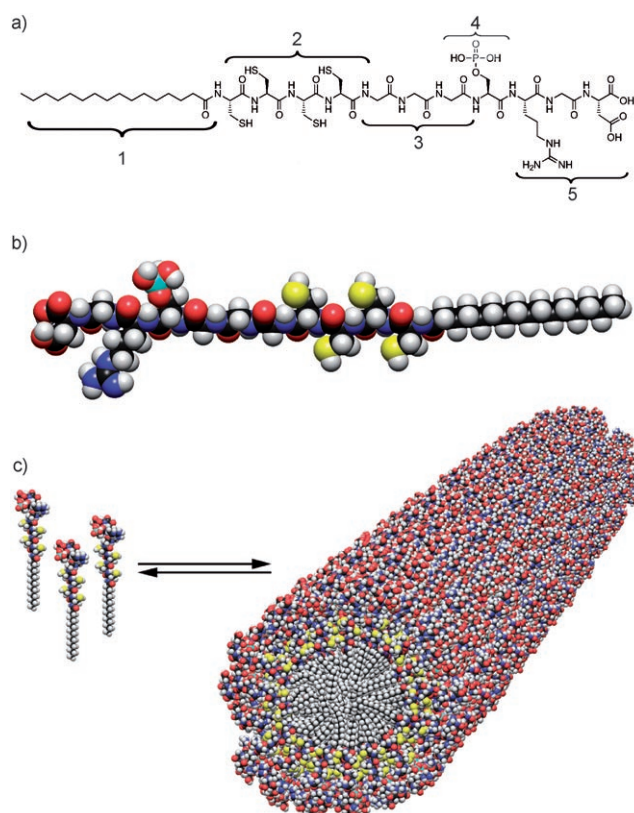


**Figure 10.** a) Chemical structure and b) molecular model of the peptide amphiphile designed by Stupp and co-workers (see text) and c) molecular model of a self-assembled cylindrical micelle. (Reprinted with permission from Ref. [180]. Copyright 2006, American Association for the Advancement of Science (AAAS).)

assembly process.<sup>[181]</sup> Related peptide amphiphiles were designed with distinct head groups based on other recognition sequences such as IKVAV and YIGSR, these being known to interact with mammalian neurons.<sup>[182]</sup> Pairs of oppositely charged peptide amphiphiles were shown to self-assemble into fibrils at neutral pH value. Fibril formation was also observed for the negatively charged molecules in acid and for positively charged molecules in base. FTIR measurements indicated significant  $\beta$ -sheet content in the fibrils. The same research group also reported the fibrillization in aqueous solution of a peptide bolamphiphile comprising two hydrophilic head groups linked by a hydrophobic spacer.<sup>[183]</sup>

Fibrillar networks based on nanotube structural elements have been observed for peptide amphiphiles.<sup>[184,185]</sup> These peptides comprised 7 or 8 residues with a charged head group of 1 or 2 amino acids and a repeated sequence of hydrophobic amino acids in the tail, for example, A<sub>6</sub>D, G<sub>6</sub>D<sub>2</sub> etc. The nanotubes were proposed to comprise a peptide bilayer similar to a lipid bilayer (the peptides were of similar length to phospholipids). TEM images showed helicity and branching of the nanotubes.<sup>[184]</sup> The same research group also reviewed other aspects of the self-assembly of amphiphilic peptides.<sup>[186]</sup> Peptide nanofibers were also observed for PAs containing 13 amino acids and an enzyme-cleavable unit, a glutamic acid to assist in calcium binding, and an RGDS cell-adhesion sequence.<sup>[187]</sup> Networks of these fibers could be enzymatically degraded. The PAs could also function as cell-growth media.

The formation of amyloid-like structures at the air/water interface was reported for “peptidolipids” with a peptide sequence based on A $\beta$ (31–35) (that is, IIGLM) attached to a C<sub>18</sub> chain.<sup>[188]</sup> Epifluorescence microscopy showed the formation of threadlike and needlelike aggregates.

Peptide amphiphiles have been prepared with DNA-binding head groups (GCN4 sequence) and C<sub>12</sub> chains terminated with polymerizable methyl methacrylate groups.<sup>[189]</sup> Fibril formation was observed in aqueous solution. A change in morphology to lamellae was observed upon binding to DNA (caused by a change in the area of the head group). Giant PAs have been prepared in which a large protein (a lipase) was conjugated to a synthetic polymer (polystyrene).<sup>[190]</sup> The end-functionalized polystyrene was linked to the protein through a disulfide bridge exposed at the surface. TEM images showed rodlike fibrillar structures.

Several types of PAs have been prepared by van Hest and co-workers. Fibril formation was observed for the peptide amphiphile C<sub>18</sub>-GANPNAAG-OH.<sup>[191]</sup> The fibrils comprised twisted  $\beta$ -sheet ribbons. Shorter N-terminally acylated peptides (C<sub>8</sub>, C<sub>10</sub>, or C<sub>12</sub> chains) showed random coil behavior independent of the temperature. Some temperature-dependent self-assembly was observed with the hydrophobic C<sub>14</sub> and C<sub>16</sub> groups, with a  $\beta$ -sheet structure observed at low temperature. These results point to the possibility to stabilize the peptide secondary structure by conjugation to a chain of appropriate length (this will be discussed further for peptide block copolymers below). The same research group have recently investigated the influence of terminal hydrophobic alkyl chains on the self-assembly of Ac-KTVIIE-NH<sub>2</sub>.<sup>[192]</sup> This hexapeptide forms  $\beta$ -sheet fibrils. The effect of alkyl chains (CH<sub>3</sub> to C<sub>16</sub>H<sub>33</sub>) at either or both termini on the stability of

fibrils was examined mainly using CD measurements. It was found that alkylation enhances the thermal stability of the peptide, as does cross-linking with PEG (see below). Furthermore, the increase in hydrophobicity leads to fibrillization at lower concentration.

The conjugation of peptides to synthetic polymers such as PEG may lead to improved solubility, enhanced stability against dilution, reduced toxicity, and immunogenicity.<sup>[193–195]</sup> A review on the self-assembly of peptide-containing block copolymers in solution can be found in Ref. [196].

In a pioneering series of reports, Meredith and co-workers have confirmed the formation of fibrils in aqueous solutions of PEG-peptide block copolymers, where the peptide block was based on the central hydrophobic domain A $\beta$ (10–35) of the  $\beta$ -amyloid peptide and the PEG block had a molar mass of 3000 g mol<sup>-1</sup>.<sup>[197–199]</sup> They found from small-angle neutron scattering (SANS) and TEM measurements that the PEG forms a coating around the fibril, and thus acts as a “steric stabilization” layer. Collier and Messersmith have investigated the effect of conjugation to PEG on the width of the peptide fibril by studying PEG-*b*-peptide and peptide-*b*-PEG-*b*-peptide copolymers containing  $\beta$ -sheet-forming sequences.<sup>[200]</sup> They investigated the secondary structure by FTIR and imaged fibrils by TEM for a peptide with 11 amino acids (and a core domain of 7 amino acids), which was designed as a transglutaminase substrate, and copolymers with terminal PEG chains or with a central PEG domain connecting two chains each of 7 amino acids.

The effect of the conjugation of PEG on the thermal and pH stability of the secondary structures formed by two classes of short peptides has been investigated by Klok and co-workers.<sup>[193,201]</sup> The first class consisted of de novo designed coiled-coil peptides<sup>[202]</sup> and the second of “switch” peptides. Switch peptides are patterned with hydrophobic and hydrophilic substituents in such a way that they can form either amphiphilic  $\alpha$  helices or amphiphilic  $\beta$  strands, depending on the pH value; the  $\beta$ -sheet structure is stable near pH 7.<sup>[203]</sup> The PEG does not disrupt the secondary structure but provides enhanced stability against variations in the concentration and pH value relative to the unconjugated peptide.<sup>[201]</sup> The self-assembly of a number of hybrid block copolymers containing amphiphilic  $\beta$ -strand sequences flanked by one or two PEG terminal chains was investigated in aqueous solution by circular dichroism spectroscopy, small-angle X-ray scattering, and transmission electron microscopy.<sup>[204]</sup> Circular dichroism measurements revealed primarily  $\beta$ -strand secondary structures. In comparison with the native peptide sequence, it was found that the secondary structure in the di- and triblock copolymers with PEG was stabilized against pH changes and temperature variation. SAXS experiments indicated the presence of fibrillar structures, and the dimensions of these were comparable to the estimated width of a  $\beta$  strand (with terminal PEG chains in the case of the copolymers). TEM studies on selectively stained and dried specimens showed directly the presence of fibrils. It was proposed that these fibrils result from the hierarchical aggregation of  $\beta$  strands into helical tapes which then stack into fibrils (see Figure 9).

Helical filaments as well as other morphologies have been observed for poly(styrene)-*b*-poly(isocyanodipeptide)

diblock copolymers.<sup>[205]</sup> The poly(isocyanide) backbones in the peptide adopt helical conformations. Self-assembly was promoted by hydrogen bonding and electrostatic interactions between the peptides.

Fibril formation has been observed for samples dried from methanol for ABA triblocks with a silklike  $\beta$ -sheet polypeptide flanked by PEG end blocks.<sup>[206]</sup> The polypeptide comprising [(AG)<sub>3</sub>EG]<sub>10</sub> is inspired by the repeated AGAG sequence found in crystalline domains of silkworm silk. The fibril morphology was influenced by the PEG chain length, with shorter fibrils being observed for the PEG with the highest molecular weight studied (5000 g mol<sup>-1</sup>).

## 10. Peptide Nanotubes

Remarkably, it has been observed that the simple dipeptide diphenylalanine forms nanotubes in aqueous solution.<sup>[207]</sup> Their formation has been ascribed to the effect of aromatic  $\pi$ - $\pi$  stacking interactions.<sup>[208,209]</sup> With the aim of testing this hypothesis, the end groups of the FF dipeptide were changed to probe whether charge has any effect on the self-assembly.<sup>[210]</sup> Variants of the original peptide NH<sub>2</sub>-FF-COOH (which has oppositely charged end groups) with uncharged end groups or with net charge also formed nanotubes or amyloid-like structures. Other aromatic dipeptides have also been shown to form nanotubes.<sup>[211]</sup> These findings underlined the important role of aromatic interactions. However, it has been pointed out that the formation of nanotubes may have alternative or additional causes. X-ray diffraction experiments suggest that the nanotube shell has the same structure as that of the single crystal,<sup>[212]</sup> thus suggesting that it is not necessary to invoke  $\pi$ - $\pi$  stacking to account for the self-assembly process in solution. The formation of hydrophobic pores in the crystal structure of several hydrophobic dipeptides<sup>[213,214]</sup> was noted before the formation of nanotubes by self-assembly was observed in solution.

The studies discussed elsewhere in this Review highlight the importance of electrostatic, hydrogen-bonding, and hydrophobic interactions in driving the self-assembly of peptides with four or more amino acids into amyloid fibrils. Tracz et al. studied variants and fragments of amylin and showed that substitution of the single aromatic residue (F) by L does not prevent amyloid formation, although it is hindered when F is substituted by A. They suggest that these results highlight the importance of hydrophobicity and  $\beta$ -sheet-forming tendency in forming fibrils.<sup>[215]</sup> Bemporad et al. investigated the effects of aromatic residues on the kinetics of aggregation of mutants of human muscle acylphosphatase by monitoring thioflavin T fluorescence.<sup>[216]</sup> The substitution of aromatic residues reduced aggregation, but this was correlated to a reduced hydrophobicity and intrinsic  $\beta$ -sheet-forming propensity rather than any specific interactions between the aromatic groups. The important role of aromatic interactions in stabilizing amyloid fibrils has also been highlighted for a synthetic peptide containing FF units<sup>[217]</sup> (this report also tabulates other studies in which aromatic interactions were implicated in amyloid formation).

X-ray diffraction studies have also provided evidence for the formation of nanotubes from peptides related to the paired helical filament morphology observed for tau and containing the sequences VQIINK and VQIVYK.<sup>[218]</sup> The hydrogen bond lies along the fibril direction with a radial peptide bilayer tube structure. Aromatic interactions between tyrosine groups of different layers stabilize the structure.

The formation of hydrogels with a fibrillar network structure has been observed for various dipeptides.<sup>[219,220]</sup> The dipeptide nanotubes have been used as templates to cast metal nanowires,<sup>[207]</sup> and other applications in bionanotechnology have been discussed.<sup>[221,222]</sup>

Ghadiri et al. pioneered the design of peptide nanotubes using stacked cyclic peptides comprising alternating D- and L-amino acids.<sup>[223]</sup> These peptides were shown to form hollow nanotubes based on a  $\beta$  helix—a structure that had been anticipated prior to their fabrication based on conformational modeling studies.<sup>[224]</sup> Figure 11 shows these structures, which have been used as artificial membrane channels<sup>[225]</sup> and may find other applications in nanotechnology.<sup>[226]</sup> A recent development has been the preparation of hybrid peptide nanotubes with a thermoresponsive poly(*N*-isopropylacrylamide) (PNIPAM) polymer shell around a cyclic peptide core.<sup>[227]</sup>

Other peptide motifs that can form nanotubes<sup>[218]</sup> include hydrophobic dipeptides in the crystal state,<sup>[214]</sup>  $\beta$ -helix-forming peptides,<sup>[228]</sup> and peptide amphiphiles/copolymers (see Section 9). The controversy over the Perutz model for the formation of nanotubes from amyloid peptides is discussed in Section 2.

## 11. Peptide Fibrillar Gels

At sufficiently high concentration, the fibrillization of peptides is accompanied by gelation. In this section we consider the structure of fibrillar hydrogels and organogels formed by several natural and synthetic peptides.

The formation of fibrils by the thermally induced denaturation of  $\beta$ -lactoglobulin and lysozyme has been discussed in Section 4.  $\beta$ -lactoglobulin forms fibrillar gels on heating at low pH values. Particulate gels are formed at higher pH values, close to the dielectric point where the protein has a low net charge.<sup>[229,230]</sup> This is outside the scope of the current Review. In regard to gel formation, it should be noted that the gels can comprise two-phase systems with nematic droplets dispersed in an isotropic phase.<sup>[231]</sup> The phase diagram has been mapped out as a function of  $\beta$ -lactoglobulin concentration and ionic strength. The persistence length of the fibrils has been obtained from rheometry measurements of the critical percolation concentration for network formation. The persistence length for  $\beta$ -lactoglobulin is much longer than that for bovine serum albumin (BSA) and ovalbumin at pH 2.<sup>[231]</sup>

In a series of papers, Ross-Murphy and co-workers have studied the formation of fibrillar gels from  $\beta$ -lactoglobulin.<sup>[116,232–234]</sup> The structure of the fibrils was probed by AFM, FTIR, and Raman spectroscopy as well as by X-ray scattering studies.<sup>[116,233,234]</sup> The mechanism of fibrillization induced by heating at pH 2 was compared to that induced by the addition

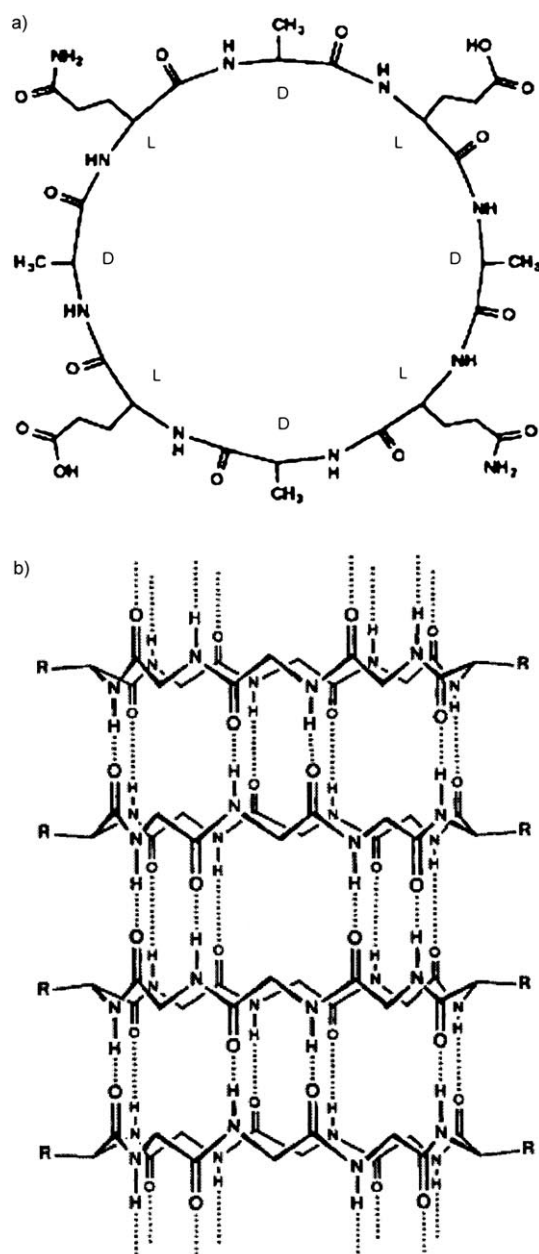


**Figure 11.** a) Cyclic peptides with alternating D- and L-amino acids, b) peptide nanotubes formed by hydrogen-bonding interactions (dotted lines) between cyclic peptides.<sup>[223]</sup>

of organic solvents such as TFE.<sup>[233]</sup> The thermally induced aggregation was more cooperative, with fibrils appearing after a definite lag period, which is consistent with a nucleation and growth mechanism, as discussed in Section 4. This relationship was also observed by rheometry studies, in particular measurements of the time dependence of the isochronal dynamic shear moduli.<sup>[116,233]</sup> The sol–gel transition boundary was mapped out as a function of concentration from time-dependent shear modulus measurements, and the scaling exponent analyzed.<sup>[234]</sup> Universal plots of gelation kinetics for curing at 75 and 80 °C were obtained by rescaling the data as  $G'/G'_{\text{inf}}$  versus  $t/t_{\text{gel}}$ , where  $G'_{\text{inf}}$  is the storage modulus extrapolated to infinite time and  $t_{\text{gel}}$  is the gel time. The pH

dependence of gelation was also investigated by similar measurements.<sup>[232]</sup> The solvent dithiothreitol can be used to denature lysozyme in an aqueous solution at high temperature. The resulting reversible gelation has been studied by shear rheometry and micro-DSC (DSC = differential scanning calorimetry), and the fibrillar morphology imaged by TEM and SEM.<sup>[235]</sup> The hydrogels act as good scaffolds for cell cultures.

Hydrogels formed by various fluorenylmethoxycarbonyl (Fmoc) protected dipeptides have been reported,<sup>[219]</sup> with the gelation of seven different dipeptides studied. Fibrillar structures were revealed by SEM, and the CD spectrum contained features associated with  $\pi$ – $\pi^*$  interactions between the fluorenyl groups and indicating the formation of helical assemblies. The use of the gels as scaffolds for cell cultures was discussed.

Hybrid hydrogels have been prepared by the self-assembly of a water-soluble synthetic polymer and coiled-coil peptides, which were genetically engineered, and expressed using *E. coli*.<sup>[236,237]</sup> A hydrophilic copolymer of *N*-(2-hydroxypropyl)methacrylamide (HPMA) and the metal-chelating monomer *N*-(*N,N'*-dicarboxymethylaminopropyl)-methacrylamide (DAMA) units was prepared. The peptides were linked through a pendant metal-chelating ligand on the DAMA unit. Two coiled-coil peptides were employed: one based on a natural sequence from the motor protein kinesin (containing a six histidine tag) and the other a block copolymer HHHHHH-*b*-(noncoiled 30 amino acid sequence)-*b*-(VSSLESK)<sub>6</sub>. The heptad sequence favors formation of coiled-coil structures and the histidine block acts as a chelating group for Ni<sup>2+</sup> ions. Hydrogels containing the wild-type peptide cross-linker underwent a volume phase transition driven by thermal unfolding. Those containing the block polypeptide did not show a volume phase transition. However, for hydrogels containing either type of cross-linker, gel swelling was observed on replacement of the histidine block by a metal-chelating ligand.<sup>[238]</sup> Peptides containing block sequences were later studied that comprised noncoiled regions (A) alternating with sequences from the kinesin stalk protein (B) with a tendency to form coiled-coil structures.<sup>[239]</sup> Histidine-tagged AB diblock, ABAB tetrablock, and ABABAB hexablock polymers were prepared by recombinant DNA techniques. Size-exclusion chromatography revealed the presence of multimer aggregate structures (mainly dimers and tetramers). The degree of swelling decreased with temperature as unfolding occurred.

The reversible formation of hydrogels from synthetic proteins containing leucine zipper coiled-coil domains in response to changes in the pH value or temperature (see Section 12) has been studied.<sup>[240]</sup> Helical secondary structure was confirmed by CD measurements, whilst diffusing wave spectroscopy (DWS) was used to probe viscoelastic properties through measurements of the mean square displacement of probe particles.

The use of synthetic polypeptide block copolymers to create hydrogels has been explored by Deming and co-workers.<sup>[241,242]</sup> They investigated the gelation of a range of diblock peptides containing a hydrophilic PLys (or poly(L-glutamic acid)) polyelectrolyte block and a hydrophobic

block based on an  $\alpha$  helix for poly(L-leucine) or a  $\beta$  sheet in the case of poly(L-valine).<sup>[241]</sup> It was found that a high degree of conformational order of the hydrophobic chain was required to observe gelation, and that the gelation was slightly better with  $\alpha$ -helical domains. The importance of chain packing was highlighted by the fact that gelation was not observed in a mixture containing racemic leucine at a concentration at which gelation occurred for a copolymer containing the enantiomeric form. Hierarchical ordering was observed with a nanoscale interpenetrating network structure and a porous bicontinuous morphology comprising a gel matrix and water channels on the microscale.<sup>[242]</sup> Laser scanning confocal microscopy and cryo-TEM measurements were used to probe the cellular network structure for a PLys-*b*-poly(L-leucine-*stat*-L-valine) diblock (Figure 12). SANS measurements confirmed a nanoscale-ordered structure.

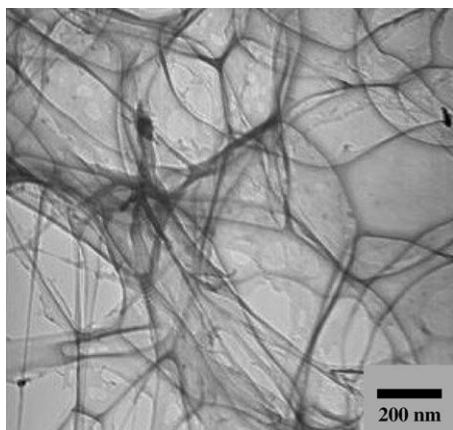


**Figure 12.** Cryo-TEM image showing the cellular structure in a gel formed by a poly(L-lysine)-*b*-poly(L-leucine-*stat*-L-valine) diblock copolymer.<sup>[242]</sup>

Pochan and co-workers have investigated the pH-dependent self-assembly of a peptide containing a <sup>D</sup>P<sup>L</sup>P (D-proline, L-proline)  $\beta$ -hairpin link between repeating VK units.<sup>[243–245]</sup> The peptide folds under basic conditions, and forms hydrogels. Folding can also be induced by increasing the ionic strength, which screens electrostatic interactions between positively charged lysine residues.<sup>[244]</sup> A variant of the original peptide was later prepared with threonine in place of several valine residues (T is less hydrophobic than V).<sup>[245]</sup> The new peptide was shown to exhibit thermally reversible hydrogelation, with gelation occurring at high temperature. Light-activated hydrogelation was later demonstrated for a homologous  $\beta$ -hairpin peptide containing an  $\alpha$ -carboxy-2-nitrobenzyl group attached through a cysteine unit.<sup>[246]</sup> Intramolecular folding was induced by exposure to UV light, and was accompanied by hydrogelation.

## 12. Fibrils from $\alpha$ Helices

There have been far fewer reports on the formation of fibrils by  $\alpha$ -helical peptides. Woolfson and co-workers have

designed so-called “SAF” (“self-assembling fibril”) peptides with coiled-coil structures based on the heptad of hydrophobic and polar residues HPPHPPP.<sup>[247–249]</sup> Complementary interactions in the core and complementary flanking ion pairs were used to create staggered heterodimers (Figure 13a).<sup>[247,250]</sup> These also had “sticky ends” to promote the formation of long fibers (Figure 13b), again as a result of interactions between charged residues.

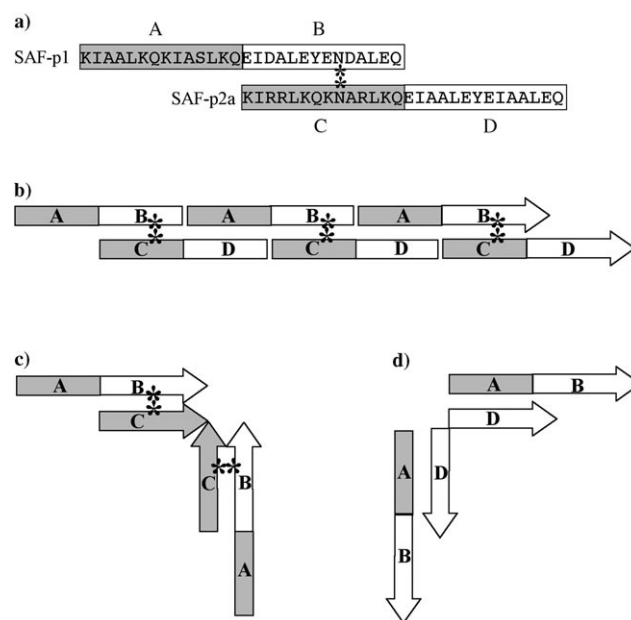


**Figure 13.** a) Self-assembly of fiber peptides through complementary electrostatic interactions within heterodimers (A with D, B with C). Interactions between the asparagine residues indicated by \* further stabilize the structures.<sup>[250]</sup> The peptides are staggered leading to the formation of fibrils (b). Kinked peptides containing flexible  $\beta$ -alanine residues (c,d) can introduce branches into the fibrils.

The design of the peptide was later improved to enhance the protofibril–protofibril interactions. Nonlinear “fiber-shaping” (FiSh) peptides were also introduced into mixed peptide systems to engineer branched fibrils (Figure 13c,d).<sup>[250,251]</sup> Hyperbranched networks as well as regularly segmented and terminated fibrils could also be produced by engineering peptides around three-arm dendritic spacers.<sup>[252]</sup> Modification of the original linear SAF peptides by substitution at the  $\epsilon$ -amino group of lysine enabled fibrils to be functionalized with ligands such as biotin or the FLAG octapeptide.<sup>[253]</sup> Both of these peptides were used to bind with streptavidin-conjugated gold nanoparticles (in the latter case biotinylated anti-FLAG antibody was required to effect recognition).

Several research groups have reported switch peptides with a design based on a dimeric parallel coiled-coil structure (known as a leucine-zipper sequence).<sup>[201,203,254–256]</sup> The use of appropriate residues in the heptad coiled-coil sequence can favor  $\beta$ -sheet formation under appropriate conditions.<sup>[203]</sup> The de novo switch peptide synthesized by Mutter et al. adopted a  $\beta$ -sheet structure at pH 4, but formed a partly  $\alpha$ -helical

structure at higher pH values. The design of Woolfson et al. contained a  $\beta$  hairpin (Figure 14).<sup>[254]</sup> Heat induced a transition from an  $\alpha$ -helix to a  $\beta$ -sheet structure that was driven by formation of intramolecular disulfide bonds between the Cys

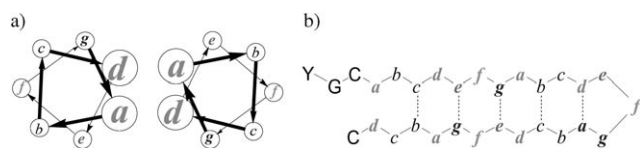


**Figure 14.** a) Helical wheel representation of a coiled-coil dimer. b) Structure of the  $\beta$ -hairpin; the interstrand hydrogen bonds are indicated by dashed lines.<sup>[254]</sup>

residues flanking the hairpin. The formation of the  $\beta$  sheets was accompanied by gelation. This was later extended to the design of related peptides which responded to chemical triggers as well as thermal processing.<sup>[257]</sup> Pagel et al. designed a 26-residue peptide that can form random coil,  $\beta$ -sheet, or coiled-coil structures at appropriate pH values or concentrations.<sup>[256]</sup> A 17-residue peptide has been designed that forms coiled-coil structures at ambient temperatures, but transforms into amyloid fibrils at high temperature.<sup>[255]</sup>

Fibril formation from a peptide containing three heptad sequences and designed to form water-soluble helix bundles was observed under appropriate pH conditions.<sup>[258]</sup> Fibers have also been observed for five-stranded fibrils of a peptide designed to associate in a staggered fashion.<sup>[259]</sup> Designed three-helix bundles have been shown to form fibrils provided the helices have an appropriate orientation.<sup>[260]</sup> The intermolecular association of the monomers is an example of a 3D domain-swapped protein structure in which one structural domain of a protein monomer is exchanged with the same domain from another protein, resulting in an intertwined oligomer.

### 13. Summary and Outlook

A clear picture is slowly emerging on the mechanism of amyloid formation by A $\beta$  and related proteins. Use of this knowledge to design inhibitors of fibrillization is underway and may lead to breakthroughs in therapies. Important questions remain on the thermodynamic basis for  $\beta$ -sheet fibrillization and its relationship to protein folding. Meanwhile, the principles of self-assembly based on noncovalent interactions are being used to design novel peptides and peptide conjugates with desired properties such as controlled fibril morphology, enhanced stability, responsive gelation, or functionalization for bio-inorganic hybrids. This is still quite a new field, and exciting new findings can be anticipated, although precise details cannot always be predicted in advance.

*I thank Dr Adam Squires (University of Reading) for useful discussions and Marta Krysmann for the TEM images used in*

*the frontispiece and Figure 2. The referees are thanked for pointing out several additional interesting references.*

Received: February 26, 2007

Published online: October 12, 2007

- [1] E. D. Eanes, G. G. Glenner, *J. Histochem. Cytochem.* **1968**, *16*, 673.
- [2] D. A. Kirschner, C. Abraham, D. J. Selkoe, *Proc. Natl. Acad. Sci. USA* **1986**, *83*, 503.
- [3] M. Sunde, C. C. F. Blake, *Adv. Protein Chem.* **1997**, *50*, 123.
- [4] L. C. Serpell, *Biochim. Biophys. Acta Mol. Basis Dis.* **2000**, *1502*, 16.
- [5] O. S. Makin, L. C. Serpell, *FEBS J.* **2005**, *272*, 5950.
- [6] D. B. Teplow, *Amyloid* **1998**, *5*, 121.
- [7] M. J. Krysmann, I. W. Hamley, P. J. F. Harris, unpublished results.
- [8] M. Goedert, M. G. Spillantini, *Science* **2006**, *314*, 777.
- [9] E. D. Roberson, L. Mucke, *Science* **2006**, *314*, 781.
- [10] J. D. Sipe, *Annu. Rev. Biochem.* **1992**, *61*, 947.
- [11] B. Caughey, P. T. Lansbury, *Annu. Rev. Neurosci.* **2003**, *26*, 267.
- [12] M. R. Chapman, L. S. Robinson, J. S. Pinkner, R. Roth, J. Heuser, M. Hammar, S. Normark, S. J. Hultgren, *Science* **2002**, *295*, 851.
- [13] J. W. Kelly, W. E. Balch, *J. Cell Biol.* **2003**, *161*, 461.
- [14] J. F. Berson, A. C. Theos, D. C. Harper, D. Tenza, G. Raposo, M. S. Marks, *J. Cell Biol.* **2003**, *161*, 521.
- [15] P. T. Lansbury, H. A. Lashuel, *Nature* **2006**, *443*, 774.
- [16] M. Bucciantini, E. Giannoni, F. Chiti, F. Baroni, L. Formigli, J. Zurdo, N. Taddei, G. Ramponi, C. M. Dobson, M. Stefani, *Nature* **2002**, *416*, 507.
- [17] F. Rousseau, J. Schmykovitz, L. Serrano, *Curr. Opin. Struct. Biol.* **2006**, *16*, 118.
- [18] C. G. Glabe, *Neurobiol. Aging* **2006**, *27*, 570.
- [19] E. Cohen, J. Bieschke, R. M. Perciavalle, J. W. Kelly, A. Dillin, *Science* **2006**, *313*, 1604.
- [20] C. M. Dobson, *Trends Biochem. Sci.* **1999**, *24*, 329.
- [21] M. Bucciantini, G. Calloni, F. Chiti, L. Formigli, D. Nosi, C. M. Dobson, M. Stefani, *J. Biol. Chem.* **2004**, *279*, 31374.
- [22] D. M. Walsh, B. P. Tseng, R. E. Rydel, M. B. Podlisny, D. J. Selkoe, *Biochemistry* **2000**, *39*, 10831.
- [23] A. Goate, M. C. Chartierharlin, M. Mullan, J. Brown, F. Crawford, L. Fidani, L. Giuffra, A. Haynes, N. Irving, L. James, R. Mant, P. Newton, K. Rooke, P. Roques, C. Talbot, M. Pericakvance, A. Roses, R. Williamson, M. Rossor, M. Owen, J. Hardy, *Nature* **1991**, *349*, 704.
- [24] R. Sherrington, E. I. Rogaev, Y. Liang, E. A. Rogaeva, G. Levesque, M. Ikeda, H. Chi, C. Lin, G. Li, K. Holman, T. Tsuda, L. Mar, J. F. Foncin, A. C. Bruni, M. P. Montesi, S. Sorbi, I. Rainero, L. Pinessi, L. Nee, I. Chumakov, D. Pollen, A. Brookes, P. Sanseau, R. J. Polinsky, W. Wasco, H. A. R. Dasilva, J. L. Haines, M. A. Pericakvance, R. E. Tanzi, A. D. Roses, P. E. Fraser, J. M. Rommens, P. H. St George-Hyslop, *Nature* **1995**, *375*, 754.
- [25] E. I. Rogaev, R. Sherrington, E. A. Rogaeva, G. Levesque, M. Ikeda, Y. Liang, H. Chi, C. Lin, K. Holman, T. Tsuda, L. Mar, S. Sorbi, B. Nacmias, S. Piacentini, L. Amaducci, I. Chumakov, D. Cohen, L. Lannfelt, P. E. Fraser, J. M. Rommens, P. H. St George-Hyslop, *Nature* **1995**, *376*, 775.
- [26] D. E. Schmechel, A. M. Saunders, W. J. Strittmatter, B. J. Crain, C. M. Hulette, S. H. Joo, M. A. Pericakvance, D. Goldgaber, A. D. Roses, *Proc. Natl. Acad. Sci. USA* **1993**, *90*, 9649.
- [27] A. M. Saunders, W. J. Strittmatter, D. Schmechel, P. H. St George-Hyslop, M. A. Pericakvance, S. H. Joo, B. L. Rosi, J. F. Gusella, D. R. Crappermaclachlan, M. J. Alberts, C.

- Hulette, B. Crain, D. Goldgaber, A. D. Roses, *Neurology* **1993**, 43, 1467.
- [28] E. H. Corder, A. M. Saunders, W. J. Strittmatter, D. E. Schmechel, P. C. Gaskell, G. W. Small, A. D. Roses, J. L. Haines, M. A. Pericakvance, *Science* **1993**, 261, 921.
- [29] K. R. Bales, T. Verina, R. C. Dodel, Y. S. Du, L. Altstiel, M. Bender, P. Hyslop, E. M. Johnstone, S. P. Little, D. J. Cummins, P. Piccardo, B. Ghetti, S. M. Paul, *Nat. Genet.* **1997**, 17, 263.
- [30] E. Rogaeva, Y. Meng, J. H. Lee, Y. Gu, T. Kawarai, F. Zou, T. Katayama, C. T. Baldwin, R. Cheng, H. Hasegawa, F. Chen, N. Shibata, K. L. Lunetta, R. Pardossi-Piquard, C. Bohm, Y. Wakutani, L. A. Cupples, K. T. Cuenco, R. C. Green, L. Pinessi, I. Rainero, S. Sorbi, A. Bruni, R. Duara, R. P. Friedland, R. Inzelberg, W. Hampe, H. Bujo, Y. Q. Song, O. M. Andersen, T. E. Willnow, N. Graff-Radford, R. C. Petersen, D. Dickson, S. D. Der, P. E. Fraser, G. Schmitt-Ulms, S. Younkin, R. Mayeux, L. A. Farrer, P. St George-Hyslop, *Nat. Genet.* **2007**, 39, 168.
- [31] T. A. Fulga, I. Elson-Schwab, V. Khurana, M. L. Steinhilb, T. L. Spires, B. T. Hyman, M. B. Feany, *Nat. Cell Biol.* **2006**, 9, 139.
- [32] C. Blake, L. C. Serpell, *Structure* **1996**, 4, 989.
- [33] J. L. Jiménez, J. L. Guijarro, E. Orlova, J. Zurdo, C. M. Dobson, M. Sunde, H. R. Saibil, *EMBO J.* **1999**, 18, 815.
- [34] J. L. Jimenez, E. J. Nettleton, M. Bouchard, C. V. Robinson, C. M. Dobson, H. R. Saibil, *Proc. Natl. Acad. Sci. USA* **2002**, 99, 9196.
- [35] D. Voet, J. G. Voet, *Biochemistry*, John Wiley & Sons, New York, **1995**.
- [36] M. Sunde, L. C. Serpell, M. Bartlam, P. E. Fraser, M. B. Pepys, C. C. F. Blake, *J. Mol. Biol.* **1997**, 273, 729.
- [37] J. D. Termine, E. D. Eanes, D. Ein, G. G. Glenner, *Biopolymers* **1972**, 11, 1103.
- [38] A. T. Petkova, Y. Ishii, J. J. Balbach, O. N. Antzutkin, R. D. Leapman, F. Delaglio, R. Tycko, *Proc. Natl. Acad. Sci. USA* **2002**, 99, 16742.
- [39] T. Lührs, C. Ritter, M. Adrian, D. Riek-Loher, B. Bohrmann, H. Döbeli, D. Schubert, R. Riek, *Proc. Natl. Acad. Sci. USA* **2005**, 102, 17342.
- [40] A. M. Squires, G. L. Devlin, S. L. Gras, A. K. Tickler, C. E. MacPhee, C. M. Dobson, *J. Am. Chem. Soc.* **2006**, 128, 11738.
- [41] M. F. Perutz, J. T. Finch, J. Berriman, A. Lesk, *Proc. Natl. Acad. Sci. USA* **2002**, 99, 5591.
- [42] P. Sikorski, E. Atkins, *Biomacromolecules* **2005**, 6, 425.
- [43] D. Sharma, L. M. Shinchuk, H. Inouye, R. Wetzel, D. A. Kirschner, *Proteins Struct. Funct. Bioinf.* **2005**, 61, 398.
- [44] H. Inouye, D. A. Kirschner in *Adv. Protein Chem.*, Vol. 73 (Eds.: A. Kakava, J. M. Squire, D. A. D. Parry), Elsevier Academic, San Diego, **2006**.
- [45] H. LeVine, *Protein Sci.* **1993**, 2, 404.
- [46] S. J. Wood, B. Maleef, T. Hart, R. Wetzel, *J. Mol. Biol.* **1996**, 256, 870.
- [47] O. S. Makin, L. C. Serpell, *Fibre Diffraction* **2004**, 12, 29.
- [48] A. Lomakin, D. S. Chung, G. B. Benedek, D. A. Kirschner, D. B. Teplow, *Proc. Natl. Acad. Sci. USA* **1996**, 93, 1125.
- [49] J. Riseman, J. G. Kirkwood, *J. Chem. Phys.* **1950**, 18, 512.
- [50] D. M. Walsh, A. Lomakin, G. B. Benedek, M. M. Condrón, D. B. Teplow, *J. Biol. Chem.* **1997**, 272, 22364.
- [51] Y. Kusumoto, A. Lomakin, D. B. Teplow, G. B. Benedek, *Proc. Natl. Acad. Sci. USA* **1998**, 95, 12277.
- [52] F. Sokolowski, A. J. Modler, R. Masuch, D. Zirwer, M. Baier, G. Lutsch, D. A. Moss, K. Gast, D. Naumann, *J. Biol. Chem.* **2003**, 278, 40481.
- [53] A. J. Modler, K. Gast, G. Lutsch, G. Damaschun, *J. Mol. Biol.* **2003**, 325, 135.
- [54] S. M. Kelly, T. J. Jess, N. C. Price, *Biochim. Biophys. Acta Proteins Proteomics* **2005**, 1751, 119.
- [55] J. Reed, A. Reed, *Anal. Biochem.* **1997**, 254, 36.
- [56] W. K. Surewicz, H. H. Mantsch, D. Chapman, *Biochemistry* **1993**, 32, 389.
- [57] B. Stuart, *Biological Applications of Infrared Spectroscopy*, Wiley, Chichester, **1997**.
- [58] H. Hiramatsu, T. Kitagawa, *Biochim. Biophys. Acta Proteins Proteomics* **2005**, 1753, 100.
- [59] M. Jackson, H. H. Mantsch, *Crit. Rev. Biochem. Mol. Biol.* **1995**, 30, 95.
- [60] P. Haris, D. Chapman, *Biopolymers* **1995**, 37, 251.
- [61] J. Kubelka, T. A. Keiderling, *J. Am. Chem. Soc.* **2001**, 123, 6142.
- [62] P. R. Costa, D. A. Kocisko, B. Q. Sun, P. T. Lansbury, R. G. Griffin, *J. Am. Chem. Soc.* **1997**, 119, 10487.
- [63] T. L. S. Benzinger, D. M. Gregory, T. S. Burkoth, H. Miller-Auer, D. G. Lynn, R. E. Botto, S. C. Meredith, *Biochemistry* **2000**, 39, 3491.
- [64] A. B. Siemer, C. Ritter, M. Ernst, R. Riek, B. H. Meier, *Angew. Chem.* **2005**, 117, 2494; *Angew. Chem. Int. Ed.* **2005**, 44, 2441.
- [65] H. Heise, W. Hoyer, S. Becker, O. C. Andronesi, D. Riedel, M. Baldus, *Proc. Natl. Acad. Sci. USA* **2005**, 102, 15871.
- [66] R. Tycko, *Curr. Opin. Struct. Biol.* **2004**, 14, 96.
- [67] R. Tycko, *Q. Rev. Biophys.* **2006**, 39, 1.
- [68] J. D. Harper, S. S. Wong, C. M. Lieber, P. T. Lansbury, *Chem. Biol.* **1997**, 4, 119.
- [69] G. Bitan, M. D. Kirkitadze, A. Lomakin, S. S. Vollers, G. B. Benedek, D. B. Teplow, *Proc. Natl. Acad. Sci. USA* **2003**, 100, 330.
- [70] C. Ha, C. B. Park, *Langmuir* **2006**, 22, 6977.
- [71] S. L. McCutchen, Z. H. Lai, G. J. Miroy, J. W. Kelly, W. Colon, *Biochemistry* **1995**, 34, 13527.
- [72] Z. Lai, W. Colón, J. W. Kelly, *Biochemistry* **1996**, 35, 6470.
- [73] G. S. Jackson, L. L. P. Hosszu, A. Power, A. F. Hill, J. Kenney, H. Saibil, C. J. Craven, J. P. Waltho, A. R. Clarke, J. Collinge, *Science* **1999**, 283, 1935.
- [74] L. L. P. Hosszu, N. J. Baxter, G. S. Jackson, A. Power, A. R. Clarke, J. P. Waltho, C. J. Craven, J. Collinge, *Nat. Struct. Biol.* **1999**, 6, 740.
- [75] M. R. Hurle, L. R. Helms, L. Li, W. Chan, R. Wetzel, *Proc. Natl. Acad. Sci. USA* **1994**, 91, 5446.
- [76] L. R. Helms, R. Wetzel, *J. Mol. Biol.* **1996**, 257, 77.
- [77] R. Raffin, L. J. Dieckman, M. Szpunar, C. Wunschl, P. R. Pokkuluri, P. Dave, P. W. Stevens, X. Y. Cai, M. Schiffer, F. J. Stevens, *Protein Sci.* **1999**, 8, 509.
- [78] S. E. Radford, C. M. Dobson, P. A. Evans, *Nature* **1992**, 358, 302.
- [79] D. R. Booth, M. Sunde, V. Bellotti, C. V. Robinson, W. L. Hutchinson, P. E. Fraser, P. N. Hawkins, C. M. Dobson, S. E. Radford, C. C. F. Blake, M. B. Pepys, *Nature* **1997**, 385, 787.
- [80] J. I. Guijarro, M. Sunde, J. A. Jones, I. D. Campbell, C. M. Dobson, *Proc. Natl. Acad. Sci. USA* **1998**, 95, 4224.
- [81] V. J. McParland, N. M. Kad, A. P. Kalverda, A. Brown, P. Kirwin-Jones, M. G. Hunter, M. Sunde, S. E. Radford, *Biochemistry* **2000**, 39, 8735.
- [82] N. M. Kad, N. H. Thomson, D. P. Smith, D. A. Smith, S. E. Radford, *J. Mol. Biol.* **2001**, 313, 559.
- [83] D. P. Smith, S. E. Radford, *Protein Sci.* **2001**, 10, 1775.
- [84] L. N. Arnaudov, R. de Vries, *Biophys. J.* **2004**, 88, 515.
- [85] F. Chiti, P. Webster, N. Taddei, A. Clark, M. Stefani, G. Ramponi, C. M. Dobson, *Proc. Natl. Acad. Sci. USA* **1999**, 96, 3590.
- [86] M. Fändrich, V. Forge, K. Buder, M. Kittler, C. M. Dobson, S. Diekmann, *Proc. Natl. Acad. Sci. USA* **2003**, 100, 15463.
- [87] R. Schweitzer-Stenner, T. Measey, A. Hagarman, F. Eker, K. Griebenow, *Biochemistry* **2006**, 45, 2810.
- [88] F. Eker, K. Griebenow, R. Schweitzer-Stenner, *Biochemistry* **2004**, 43, 6893.
- [89] L. M. Hou, H. Y. Shao, Y. B. Zhang, H. Li, N. K. Menon, E. B. Neuhaus, J. M. Brewer, I. J. L. Byeon, D. G. Ray, M. P. Vitek, T.

- Iwashita, R. A. Makula, A. B. Przybyla, M. G. Zagorski, *J. Am. Chem. Soc.* **2004**, *126*, 1992.
- [90] C. D. Syme, E. W. Blanch, C. Holt, R. Jakes, M. Goedert, L. Hecht, L. D. Barron, *Eur. J. Biochem.* **2002**, *269*, 148.
- [91] S. Narayanan, B. Reif, *Biochemistry* **2005**, *44*, 1444.
- [92] M. Tanaka, Y. Machida, Y. Nishikawa, T. Akagi, T. Hashikawa, T. Fujisawa, N. Nukina, *J. Biol. Chem.* **2003**, *278*, 34717.
- [93] G. P. Bates, C. Benn in *Huntington's Disease* (Eds.: G. P. Bates, P. S. Harper, L. Jones), Oxford University Press, Oxford, **2002**.
- [94] M. Calamai, C. Canale, A. Relini, M. Stefani, F. Chiti, C. M. Dobson, *J. Mol. Biol.* **2005**, *346*, 603.
- [95] J. T. Jarrett, P. T. Lansbury, *Cell* **1993**, *73*, 1055.
- [96] J. D. Harper, P. T. Lansbury, *Annu. Rev. Biochem.* **1997**, *66*, 385.
- [97] J. N. Israelachvili, *Intermolecular and Surface Forces*, Academic Press, San Diego, **1991**.
- [98] J. M. Andreu, S. N. Timasheff, *Methods Enzymol.* **1986**, *130*, 47.
- [99] K. Johan, G. Westermark, U. Engström, A. Gustavsson, P. Hultman, P. Westermark, *Proc. Natl. Acad. Sci. USA* **1998**, *95*, 2558.
- [100] C. M. Dobson, *Nature* **2003**, *426*, 884.
- [101] I. V. Baskakov, G. Legname, Z. Gryczynski, S. B. Prusiner, *Protein Sci.* **2004**, *13*, 586.
- [102] L. N. Arnaudov, R. de Vries, *Biomacromolecules* **2003**, *4*, 1614.
- [103] Y.-H. Chen, J. T. Yang, H. M. Martinez, *Biochemistry* **1972**, *11*, 4120.
- [104] Y.-H. Chen, J. T. Yang, K. H. Chau, *Biochemistry* **1974**, *13*, 3350.
- [105] P. Aymard, T. Nicolai, D. Durand, A. Clark, *Macromolecules* **1999**, *32*, 2542.
- [106] L. N. Arnaudov, R. de Vries, *Biomacromolecules* **2006**, *7*, 3490.
- [107] M. R. H. Krebs, D. K. Wilkins, E. W. Chung, M. C. Pitkeathly, A. K. Chamberlain, J. Zurdo, C. V. Robinson, C. M. Dobson, *J. Mol. Biol.* **2000**, *300*, 541.
- [108] E. K. Hill, B. Krebs, D. G. Goodall, G. J. Howlett, D. E. Dunstan, *Biomacromolecules* **2006**, *7*, 10.
- [109] V. Castelletto, I. W. Hamley, *Biomacromolecules* **2007**, *8*, 77.
- [110] W. P. Esler, E. R. Stimson, J. R. Ghilardi, H. V. Vinters, J. P. Lee, P. W. Mantyh, J. E. Maggio, *Biochemistry* **1996**, *35*, 749.
- [111] H. Naiki, K. Nakakuki, *Lab. Invest.* **1996**, *74*, 374.
- [112] S. R. Collins, A. Douglass, R. D. Vale, J. S. Weissman, *PLoS Biol.* **2004**, *2*, 1582.
- [113] S. Narayanan, S. Walter, B. Reif, *ChemBioChem* **2006**, *7*, 757.
- [114] M. R. H. Krebs, L. A. Morozova-Roche, K. Daniel, C. V. Robinson, C. M. Dobson, *Protein Sci.* **2004**, *13*, 1933.
- [115] A. T. Petkova, R. D. Leapman, Z. H. Guo, W. M. Yau, M. P. Mattson, R. Tycko, *Science* **2005**, *307*, 262.
- [116] W. S. Gosal, A. H. Clark, P. D. A. Pudney, S. B. Ross-Murphy, *Langmuir* **2002**, *18*, 7174.
- [117] T. Ban, D. Hamada, K. Hasegawa, H. Naiki, Y. Goto, *J. Biol. Chem.* **2003**, *278*, 16462.
- [118] M. P. Lambert, A. K. Barlow, B. A. Chromy, C. Edwards, R. Freed, M. Liosatos, T. E. Morgan, I. Rozovsky, B. Trommer, K. L. Viola, P. Wals, C. Zhang, C. E. Finch, G. A. Krafft, W. L. Klein, *Proc. Natl. Acad. Sci. USA* **1998**, *95*, 6448.
- [119] K. N. Dahlgren, A. M. Manelli, W. B. Stine, L. K. Baker, G. A. Krafft, M. J. LaDu, *J. Biol. Chem.* **2002**, *277*, 32046.
- [120] D. M. Hartley, D. M. Walsh, C. P. P. Ye, T. Diehl, S. Vasquez, P. M. Vassilev, D. B. Teplow, D. J. Selkoe, *J. Neurosci.* **1999**, *19*, 8876.
- [121] K. Andersson, A. Olofsson, E. H. Nielsen, S. E. Svehag, E. Lundgren, *Biochem. Biophys. Res. Commun.* **2002**, *294*, 309.
- [122] R. Kaye, E. Head, J. L. Thompson, T. M. McIntire, S. C. Milton, C. W. Cotman, C. G. Glabe, *Science* **2003**, *300*, 486.
- [123] Y. Zhang, R. McLaughlin, C. Goodyer, A. LeBlanc, *J. Cell Biol.* **2002**, *156*, 519.
- [124] J. P. Cleary, D. M. Walsh, J. J. Hofmeister, G. M. Shankar, M. A. Kuskowski, D. J. Selkoe, K. H. Ashe, *Nat. Neurosci.* **2005**, *8*, 79.
- [125] Y. S. Du, X. Wei, R. Dodel, N. Sommer, H. Hampel, F. Gao, Z. Z. Ma, L. M. Zhao, W. H. Oertel, M. Farlow, *Brain* **2003**, *126*, 1935.
- [126] M. P. Lambert, K. L. Viola, B. A. Chromy, L. Chang, T. E. Morgan, J. X. Yu, D. L. Venton, G. A. Krafft, C. E. Finch, W. L. Klein, *J. Neurochem.* **2001**, *79*, 595.
- [127] S. Lesné, M. T. Koh, L. Kotilinek, R. Kaye, C. G. Glabe, A. Yang, M. Gallagher, K. H. Ashe, *Nature* **2006**, *440*, 352.
- [128] H. B. Pollard, N. Arispe, E. Rojas, *Cell. Mol. Neurobiol.* **1995**, *15*, 513.
- [129] J. I. Kourie, C. L. Henry, *Clin. Exp. Pharmacol. Physiol.* **2002**, *29*, 741.
- [130] H. A. Lashuel, D. Hartley, B. M. Petre, T. Walz, P. T. Lansbury, *Nature* **2002**, *418*, 291.
- [131] N. Arispe, E. Rojas, H. B. Pollard, *Proc. Natl. Acad. Sci. USA* **1993**, *90*, 567.
- [132] N. Arispe, H. B. Pollard, E. Rojas, *Proc. Natl. Acad. Sci. USA* **1993**, *90*, 10573.
- [133] N. Arispe, H. B. Pollard, E. Rojas, *Proc. Natl. Acad. Sci. USA* **1996**, *93*, 1710.
- [134] Y. Hirakura, M. C. Lin, B. L. Kagan, *J. Neurosci. Res.* **1999**, *57*, 458.
- [135] H. Lin, R. Bhatia, R. Lal, *FASEB J.* **2001**, *15*, 2433.
- [136] M. J. Volles, P. T. Lansbury, *Biochemistry* **2002**, *41*, 4595.
- [137] T. R. Jahn, S. E. Radford, *FEBS J.* **2005**, *272*, 5962.
- [138] M. Balbirnie, R. Grothe, D. S. Eisenberg, *Proc. Natl. Acad. Sci. USA* **2001**, *98*, 2375.
- [139] B. Gaughey, G. S. Baron, *Nature* **2006**, *443*, 803.
- [140] M. Fändrich, C. M. Dobson, *EMBO J.* **2002**, *21*, 5682.
- [141] W. K. Kim, M. H. Hecht, *Proc. Natl. Acad. Sci. USA* **2006**, *103*, 15824.
- [142] W. J. Goux, L. Kopplin, A. D. Nguyen, K. Leak, M. Rutkowsky, V. D. Shanmuganandam, D. Sharma, H. Inouye, D. A. Kirschner, *J. Biol. Chem.* **2004**, *279*, 26868.
- [143] M. Reches, E. Gazit, *Amyloid* **2004**, *11*, 81.
- [144] M. Reches, Y. Porat, E. Gazit, *J. Biol. Chem.* **2002**, *277*, 35475.
- [145] C. Hilbich, B. Kisterswoike, J. Reed, C. L. Masters, K. Beyreuther, *J. Mol. Biol.* **1992**, *228*, 460.
- [146] L. O. Tjernberg, J. Naslund, F. Lindqvist, J. Johansson, A. R. Karlstrom, J. Thyberg, L. Terenius, C. Nordstedt, *J. Biol. Chem.* **1996**, *271*, 8545.
- [147] L. O. Tjernberg, C. Lilliehook, D. J. E. Callaway, J. Naslund, S. Hahne, J. Thyberg, L. Terenius, C. Nordstedt, *J. Biol. Chem.* **1997**, *272*, 12601.
- [148] M. A. Findeis, G. M. Musso, C. C. Arico-Muendel, H. W. Benjamin, A. M. Hundal, J. J. Lee, J. Chin, M. Kelley, J. Wakefield, N. J. Hayward, S. M. Molineaux, *Biochemistry* **1999**, *38*, 6791.
- [149] L. O. Tjernberg, D. J. E. Callaway, A. Tjernberg, S. Hahne, C. Lilliehook, L. Terenius, J. Thyberg, C. Nordstedt, *J. Biol. Chem.* **1999**, *274*, 12619.
- [150] D. J. Gordon, R. Tappe, S. C. Meredith, *J. Pept. Res.* **2002**, *60*, 37.
- [151] D. J. Gordon, K. L. Sciarretta, S. C. Meredith, *Biochemistry* **2001**, *40*, 8237.
- [152] C. Soto, E. M. Sigurdsson, L. Morelli, R. A. Kumar, E. M. Castano, B. Frangione, *Nat. Med.* **1998**, *4*, 822.
- [153] G. Zhang, M. J. Leibowitz, P. J. Sinko, S. Stein, *Bioconjugate Chem.* **2003**, *14*, 86.
- [154] J. J. Balbach, Y. Ishii, O. N. Antzutkin, R. D. Leapman, N. W. Rizzo, F. Dyda, J. Reed, R. Tycko, *Biochemistry* **2000**, *39*, 13748.
- [155] K. Lu, J. Jacob, P. Thiyagarajan, V. P. Conticello, D. G. Lynn, *J. Am. Chem. Soc.* **2003**, *125*, 6391.
- [156] S. J. Wood, R. Wetzel, J. D. Martin, M. R. Hurle, *Biochemistry* **1995**, *34*, 724.
- [157] A.-M. Fernandez-Escamilla, F. Rousseau, J. Schymkowitz, L. Serrano, *Nat. Biotechnol.* **2004**, *22*, 1302.

- [158] A. P. Pawar, K. F. DuBay, J. Zurdo, F. Chiti, M. Vendruscolo, C. M. Dobson, *J. Mol. Biol.* **2005**, *350*, 379.
- [159] Y. Kallberg, M. Gustafsson, B. Persson, J. Thyberg, J. Johansson, *J. Biol. Chem.* **2001**, *276*, 12945.
- [160] A. A. Watson, D. P. Fairlie, D. J. Craik, *Biochemistry* **1998**, *37*, 12700.
- [161] H. Sticht, P. Bayer, D. Willbold, S. Dames, C. Hilbich, K. Beyreuther, R. W. Frank, P. Rosch, *Eur. J. Biochem.* **1995**, *233*, 293.
- [162] M. Coles, W. Bicknell, A. A. Watson, D. P. Fairlie, D. J. Craik, *Biochemistry* **1998**, *37*, 11064.
- [163] S. B. Malinchik, H. Inouye, K. E. Szumowski, D. A. Kirschner, *Biophys. J.* **1998**, *74*, 537.
- [164] A. Aggeli, M. Bell, N. Boden, J. N. Keen, P. F. Knowles, T. C. B. McLeish, M. Pitkeathly, S. E. Radford, *Nature* **1997**, *386*, 259.
- [165] A. Aggeli, M. L. Bannister, M. Bell, N. Boden, J. B. C. Findlay, M. Hunter, P. F. Knowles, J.-C. Yang, *Biochemistry* **1998**, *37*, 8121.
- [166] A. Aggeli, M. Bell, N. Boden, J. N. Keen, T. C. B. McLeish, I. Nyrkova, S. E. Radford, A. Semenov, *J. Mater. Chem.* **1997**, *7*, 1135.
- [167] A. Aggeli, G. Fytas, D. Vlassopoulos, T. C. B. McLeish, P. J. Mawer, N. Boden, *Biomacromolecules* **2001**, *2*, 378.
- [168] I. A. Nyrkova, A. N. Semenov, A. Aggeli, M. Bell, N. Boden, T. C. B. McLeish, *Eur. Phys. J. B* **2000**, *17*, 499.
- [169] A. Aggeli, I. A. Nyrkova, M. Bell, R. Harding, L. Carrick, T. C. B. McLeish, A. N. Semenov, N. Boden, *Proc. Natl. Acad. Sci. USA* **2001**, *98*, 11857.
- [170] L. Carrick, M. Tassieri, T. A. Waigh, A. Aggeli, N. Boden, C. Bell, J. Fisher, E. Ingham, R. M. L. Evans, *Langmuir* **2005**, *21*, 3733.
- [171] A. Aggeli, M. Bell, N. Boden, L. M. Carrick, A. E. Strong, *Angew. Chem.* **2003**, *115*, 5761; *Angew. Chem. Int. Ed.* **2003**, *42*, 5603.
- [172] A. Aggeli, M. Bell, N. Boden, L. Carrick, C. W. G. Fishwick, P. J. Mawer, S. E. Radford, A. E. Strong, *J. Am. Chem. Soc.* **2003**, *125*, 9619.
- [173] M. L. de la Paz, K. Goldie, J. Zurdo, E. Lacroix, C. M. Dobson, A. Hoenger, L. Serrano, *Proc. Natl. Acad. Sci. USA* **2002**, *99*, 16052.
- [174] P. Chen, *Colloids Surf. A* **2005**, *261*, 3.
- [175] S. Jun, Y. Hong, H. Imamura, B.-Y. Ha, J. Bechhoefer, P. Chen, *Biophys. J.* **2004**, *87*, 1249.
- [176] H. Yang, M. Pritzker, S. Y. Fung, Y. Sheng, W. Wang, P. Chen, *Langmuir* **2006**, *22*, 8553.
- [177] K. Pagel, T. Vagt, T. Kohajda, B. Kokschi, *Org. Biomol. Chem.* **2005**, *3*, 2500.
- [178] K. Pagel, T. Vagt, B. Kokschi, *Org. Biomol. Chem.* **2005**, *3*, 3843.
- [179] S. Matsumura, S. Uemura, H. Mihara, *Chem. Eur. J.* **2004**, *10*, 2789.
- [180] J. D. Hartgerink, E. Beniash, S. I. Stupp, *Science* **2001**, *294*, 1684.
- [181] J. D. Hartgerink, E. Beniash, S. I. Stupp, *Proc. Natl. Acad. Sci. USA* **2002**, *99*, 5133.
- [182] K. L. Niece, J. D. Hartgerink, J. J. M. Donners, S. I. Stupp, *J. Am. Chem. Soc.* **2003**, *125*, 7146.
- [183] R. C. Claussen, B. M. Rabatic, S. I. Stupp, *J. Am. Chem. Soc.* **2003**, *125*, 12680.
- [184] S. Vauthey, S. Santoso, H. Gong, N. Watson, S. Zhang, *Proc. Natl. Acad. Sci. USA* **2002**, *99*, 5355.
- [185] S. Santoso, W. Hwang, H. Hartman, S. Zhang, *Nano Lett.* **2002**, *2*, 687.
- [186] S. S. Santoso, S. Vauthey, S. Zhang, *Curr. Opin. Colloid Interface Sci.* **2002**, *7*, 262.
- [187] H.-W. Jun, V. Yuwono, S. E. Paramonov, J. D. Hartgerink, *Adv. Mater.* **2005**, *17*, 2612.
- [188] C. Li, J. Orbulescu, G. Sui, R. M. Leblanc, *Langmuir* **2004**, *20*, 8641.
- [189] R. Bitton, J. Schmidt, M. Biesalski, R. Tu, M. Tirrell, H. Bianco-Peled, *Langmuir* **2005**, *21*, 11888.
- [190] K. Velonia, A. E. Rowan, R. J. M. Nolte, *J. Am. Chem. Soc.* **2002**, *124*, 4224.
- [191] D. W. P. M. Löwik, J. Garcia-Hartjes, J. T. Meijer, J. C. M. van Hest, *Langmuir* **2005**, *21*, 524.
- [192] J. T. Meijer, M. Roeters, V. Viola, D. W. P. M. Löwik, G. Vriend, J. C. M. van Hest, *Langmuir* **2007**, *23*, 2058.
- [193] G. W. M. Vandermeulen, C. Tziatzios, H.-A. Klok, *Macromolecules* **2003**, *36*, 4107.
- [194] G. W. M. Vandermeulen, H.-A. Klok, *Macromol. Biosci.* **2004**, *4*, 383.
- [195] I. W. Hamley, *Block Copolymers in Solution*, Wiley, Chichester, **2005**.
- [196] H. Schlaad, *Adv. Polym. Sci.* **2006**, *202*, 53.
- [197] T. S. Burkoth, T. L. S. Benzinger, D. N. M. Jones, K. Hallenga, S. C. Meredith, D. G. Lynn, *J. Am. Chem. Soc.* **1998**, *120*, 7655.
- [198] T. S. Burkoth, T. L. S. Benzinger, V. Urban, D. G. Lynn, S. C. Meredith, P. Thiyagarajan, *J. Am. Chem. Soc.* **1999**, *121*, 7429.
- [199] P. Thiyagarajan, T. S. Burkoth, V. Urban, S. Seifert, T. L. S. Benzinger, D. M. Morgan, D. Gordon, S. C. Meredith, D. G. Lynn, *J. Appl. Crystallogr.* **2000**, *33*, 535.
- [200] J. H. Collier, P. B. Messersmith, *Adv. Mater.* **2004**, *16*, 907.
- [201] H.-A. Klok, G. W. M. Vandermeulen, H. Nuhn, A. Rösler, I. W. Hamley, V. Castelletto, H. Xu, S. Sheiko, *Faraday Discuss.* **2005**, *128*, 29.
- [202] J. Y. Su, R. S. Hodges, C. M. Kay, *Biochemistry* **1994**, *33*, 15501.
- [203] M. Mutter, R. Gassmann, U. Buttkeus, K.-H. Altmann, *Angew. Chem.* **1991**, *103*, 1504; *Angew. Chem. Int. Ed. Engl.* **1991**, *30*, 1514.
- [204] I. W. Hamley, I. A. Ansari, V. Castelletto, H. Nuhn, A. Rösler, H.-A. Klok, *Biomacromolecules* **2005**, *6*, 1310.
- [205] J. J. L. M. Cornelissen, M. Fischer, N. A. J. M. Sommerdijk, R. J. M. Nolte, *Science* **1998**, *280*, 1427.
- [206] J. M. Smeenk, P. Schön, M. B. J. Otten, S. Speller, H. G. Stunnenberg, J. C. M. van Hest, *Macromolecules* **2006**, *39*, 2989.
- [207] M. Reches, E. Gazit, *Science* **2003**, *300*, 625.
- [208] E. Gazit, *FEBS J.* **2005**, *272*, 5971.
- [209] S. Gilead, E. Gazit, *Supramol. Chem.* **2005**, *17*, 87.
- [210] M. Reches, E. Gazit, *Isr. J. Chem.* **2005**, *45*, 363.
- [211] M. Reches, E. Gazit, *Nano Lett.* **2004**, *4*, 581.
- [212] C. H. Görbitz, *Chem. Commun.* **2006**, 2332.
- [213] C. H. Görbitz, *Chem. Eur. J.* **2001**, *7*, 5153.
- [214] C. H. Görbitz, *New J. Chem.* **2003**, *27*, 1789.
- [215] S. M. Tracz, A. Abedini, M. Driscoll, D. P. Raleigh, *Biochemistry* **2004**, *43*, 15901.
- [216] F. Bemporad, N. Taddei, M. Stefani, F. Chiti, *Protein Sci.* **2006**, *15*, 862.
- [217] O. S. Makin, E. Atkins, P. Sikorski, J. Johansson, L. C. Serpell, *Proc. Natl. Acad. Sci. USA* **2005**, *102*, 315.
- [218] H. Inouye, D. Sharma, W. J. Goux, D. A. Kirschner, *Biophys. J.* **2005**, *90*, 1774.
- [219] V. Jayawarna, M. Ali, T. A. Jowitt, A. F. Miller, A. Saiani, J. E. Gough, R. V. Ulijn, *Adv. Mater.* **2006**, *18*, 611.
- [220] A. Mahler, M. Reches, M. Rechter, S. Cohen, E. Gazit, *Adv. Mater.* **2006**, *18*, 1365.
- [221] M. Yemini, M. Reches, J. Rishpon, E. Gazit, *Nano Lett.* **2004**, *4*, 183.
- [222] X. Gao, H. Matsui, *Adv. Mater.* **2005**, *17*, 2037.
- [223] M. R. Ghadiri, J. R. Granja, R. A. Milligan, D. E. McRee, N. Khazanovich, *Nature* **1993**, *366*, 324.
- [224] P. De Santis, S. Morosetti, R. Rizzo, *Macromolecules* **1974**, *7*, 52.
- [225] M. R. Ghadiri, J. R. Granja, L. K. Buehler, *Nature* **1994**, *369*, 301.

- [226] D. T. Bong, T. D. Clark, J. R. Granja, M. R. Ghadiri, *Angew. Chem.* **2001**, *113*, 1016; *Angew. Chem. Int. Ed.* **2001**, *40*, 988.
- [227] J. Couet, J. D. J. S. Samuel, A. Kopyshv, S. Santer, M. Biesalski, *Angew. Chem.* **2005**, *117*, 3361; *Angew. Chem. Int. Ed.* **2005**, *44*, 3297.
- [228] C. Valery, M. Paternostre, B. Robert, T. Gulik-Krzywicki, T. Narayanan, J. C. Dedieu, G. Keller, M. L. Torres, R. Cherif-Cheikh, P. Calvo, F. Artzner, *Proc. Natl. Acad. Sci. USA* **2003**, *100*, 10258.
- [229] R. Parker, T. E. Noel, G. J. Brownsey, K. Laos, S. G. Ring, *Biophys. J.* **2005**, *89*, 1227.
- [230] E. H. C. Bromley, M. R. H. Krebs, A. M. Donald, *Eur. Phys. J. E* **2006**, *21*, 145.
- [231] L. M. C. Sagis, C. Veerman, E. van der Linden, *Langmuir* **2004**, *20*, 924.
- [232] G. M. Kavanagh, A. H. Clark, S. B. Ross-Murphy, *Langmuir* **2000**, *16*, 9584.
- [233] W. S. Gosal, A. H. Clark, S. B. Ross-Murphy, *Biomacromolecules* **2004**, *5*, 2408.
- [234] W. S. Gosal, A. H. Clark, S. B. Ross-Murphy, *Biomacromolecules* **2004**, *5*, 2420.
- [235] H. Yan, A. Saiani, J. E. Gough, A. F. Miller, *Biomacromolecules* **2006**, *7*, 2776.
- [236] C. Wang, R. J. Stewart, J. Kopecek, *Nature* **1999**, *397*, 417.
- [237] J. Kopecek, A. Tang, C. Wang, R. J. Stewart, *Macromol. Symp.* **2001**, *174*, 31.
- [238] A. Tang, C. Wang, R. J. Stewart, J. Kopecek, *J. Controlled Release* **2001**, *72*, 57.
- [239] C. Wang, J. Kopecek, R. J. Stewart, *Biomacromolecules* **2001**, *2*, 912.
- [240] W. A. Petka, J. L. Harden, K. P. McGrath, D. Wirtz, D. A. Tirrell, *Science* **1998**, *281*, 389.
- [241] A. P. Nowak, V. Breedveld, L. Pakstis, B. Ozbas, D. J. Pine, D. Pochan, T. J. Deming, *Nature* **2002**, *417*, 424.
- [242] D. J. Pochan, L. Pakstis, B. Ozbas, A. P. Nowak, T. J. Deming, *Macromolecules* **2002**, *35*, 5358.
- [243] J. P. Schneider, D. J. Pochan, B. Ozbas, K. Rajogopal, L. Pakstis, J. Kretsinger, *J. Am. Chem. Soc.* **2002**, *124*, 15030.
- [244] B. Ozbas, J. Kretsinger, K. Rajogopal, J. P. Schneider, D. J. Pochan, *Macromolecules* **2004**, *37*, 7331.
- [245] D. J. Pochan, J. P. Schneider, J. Kretsinger, B. Ozbas, K. Rajogopal, L. Haines, *J. Am. Chem. Soc.* **2003**, *125*, 11802.
- [246] L. A. Haines, K. Rajogopal, B. Ozbas, D. A. Salick, D. J. Pochan, J. P. Schneider, *J. Am. Chem. Soc.* **2005**, *127*, 17025.
- [247] M. J. Pandya, G. M. Spooner, M. Sunde, J. R. Thorpe, A. Rodger, D. N. Woolfson, *Biochemistry* **2000**, *39*, 8728.
- [248] C. E. MacPhee, D. N. Woolfson, *Curr. Opin. Solid State Mater. Sci.* **2004**, *8*, 141.
- [249] D. N. Woolfson, *Adv. Protein Chem.* **2005**, *70*, 79.
- [250] M. G. Ryadnov, D. N. Woolfson, *Nat. Mater.* **2003**, *2*, 329.
- [251] M. G. Ryadnov, D. N. Woolfson, *Angew. Chem.* **2003**, *115*, 3129; *Angew. Chem. Int. Ed.* **2003**, *42*, 3021.
- [252] M. G. Ryadnov, D. N. Woolfson, *J. Am. Chem. Soc.* **2005**, *127*, 12407.
- [253] M. G. Ryadnov, D. N. Woolfson, *J. Am. Chem. Soc.* **2004**, *126*, 7454.
- [254] B. Ciani, E. G. Hutchinson, R. B. Sessions, D. N. Woolfson, *J. Biol. Chem.* **2002**, *277*, 10150.
- [255] R. A. Kammerer, D. Kostrewa, J. Zurdo, A. Detken, C. Garcia-Echeverria, J. D. Green, S. A. Muller, B. H. Meier, F. K. Winkler, C. M. Dobson, M. O. Steinmetz, *Proc. Natl. Acad. Sci. USA* **2004**, *101*, 4435.
- [256] K. Pagel, S. C. Wagner, K. Samedov, H. von Berlepsch, C. Bottcher, B. Koks, *J. Am. Chem. Soc.* **2006**, *128*, 2196.
- [257] M. J. Pandya, E. Cerasoli, A. Joseph, R. G. Stoneman, E. Waite, D. N. Woolfson, *J. Am. Chem. Soc.* **2004**, *126*, 17016.
- [258] S. Kojima, Y. Kuriki, T. Yoshida, K. Yazaki, K. Miura, *Proc. Jpn. Acad. Ser. B* **1997**, *73*, 7.
- [259] S. A. Potekhin, T. N. Melnik, V. Popov, N. F. Lanina, A. A. Vazina, P. Rigler, A. S. Verdini, G. Corradin, A. V. Kajava, *Chem. Biol.* **2001**, *8*, 1025.
- [260] N. L. Ogiwara, G. Ghirlanda, J. W. Bryson, M. Gingery, W. F. DeGrado, D. Eisenberg, *Proc. Natl. Acad. Sci. USA* **2001**, *98*, 1404.